Networked Control of Polynomial Fuzzy Systems with Time-Delay Based on Piecewise Lyapunov Functions

Gwo-Ruey Yu, *Member, IEEE*, Chen-Chih Chung

***Abstract*—**This thesis studied the networked control systems (NCSs) of polynomial fuzzy time-delay systems based on piecewise polynomial Lyapunov functions (PPLF), and applied them to the path tracking control of mobile robots and quadrotors. The number of fuzzy rules could be reduced to two by using the novel modeling method, which greatly reduces the hardware cost. Both mobile robots and quadrotors had the problem of time delay in the plant. The time delay system developed in this work could tolerate the time delay of the plant through the modeling method of calculating the time delay of the plant additionally. The Lyapunov-Krasovskii piecewise polynomial functional function was designed using the minimum-type polynomial Lyapunov piecewise function. By reducing the stable condition number, the gain solution space could be expanded, and then the performance of the controller was better than the existing polynomial fuzzy network. Since the number of stable conditions was less than the existing methods, the proposed method could also expand the feasible solution space and obtain better controller performance compared with the general Lyapunov function controller. Thus, based on the piecewise polynomial Lyapunov-Krasovskii function, considering the time delay and package dropout caused by the network, a robust stability condition is proposed in this work with calculated time delay in the SOS-based relaxation stabilization condition, and an SOS-based formation relaxation condition. The theorems proposed in this work consider the network-caused package dropout and time delay. Theorem 1 additionally considers the time delay of the plant and then simulates the virtual model of the mobile robot and the quadrotor to verify that the proposed theorem can be applied to the controller resisting external disturbances, it tolerates model uncertainty and formation effectiveness. Finally, the designed network controller was used for the path tracking of the mobile robot and the quadrotor, and the performance of the theorem proposed in this work was verified to be better than the existing controller.

***Index Terms*—novel polynomial fuzzy, piecewise polynomial Lyapunov functions, networked control time-delay systems, polynomial formation control.**

I. Introduction

There has been a rapid development in artificial intelligence and the Internet of Things. Intelligent automation is replacing the existing human structure at a visible rate and is widely used in various regions [1, 2]. NCSs can perform many tasks over long distances because they are connected to cyberspace and physical space. Furthermore, NCSs are implemented using a shared network, which eliminates unnecessary wiring, reduces complexity and reduces setup and design costs. The main structure of the system can also be changed at a lower cost by adding sensors, controllers, or actuators, which makes NCSs even more important.

The cloud server, in addition to serving as a communication platform between networks, can also perform sufficient computing for devices that require a large amount of computing power. With features such as high speed, low latency, and multiple connections, the 5G network can transmit more packages simultaneously, send the signal back to the cloud server in real-time, and can quickly respond in the event of an emergency, with low-latency support [3]. Therefore, 5G network technology is becoming increasingly practical. However, due to the addition of the network and the uncertainty of the communication channel, transmission time delay and package dropout problems must exist in the data transmission process. Network control is a very effective solution. The Lyapunov-Krasovskii function is a popular method to study system stability problems with time delays [4-7].

In the real world, most systems are nonlinear, in part to solve the problem of designing difficult controllers. Takagi-Sasuke (T-S) fuzzy logic control [8-11] uses multiple linear subsystems to approximate nonlinear systems by locally linearizing them efficiently through the IF-THEN fuzzy rule. However, even with the design method being general, with a complex system, it can be difficult to determine the appropriate gain through linear matrix inequality (LMI). To reduce fuzzy rules, Tanaka proposed an SOS-based polynomial fuzzy control system [12-14]. This allows polynomials and state variables to be included in model rules, as well as polynomial matrix elements in the system matrix. When compared with the T-S fuzzy control system, it also solves the problem of having too many fuzzy rules and only allowing constants in the system matrix elements. In this regard, the polynomial fuzzy time-delay control system based on SOS stability conditions can reduce subsystems and the number of fuzzy rules. Compared with the T-S fuzzy control systems, the polynomial fuzzy time-delay control system can generate a larger feasible solution space and achieve improved control performance when solving the control gain problem. The T-S fuzzy control system is a special case of the polynomial fuzzy control system since the polynomial fuzzy NCSs can contain polynomials in its fuzzy model.

Generally, the quadratic Lyapunov function is used to derive stability conditions for polynomial fuzzy control systems. The control performance derived by SOS derivation using a single quadratic Lyapunov function for stability analysis is too conservative [15-18]. Consequently, we can relax the stability conditions when using a stability analysis method that uses PPLFs; these functions can be further subdivided into

Gwo-Ruey Yu is with Department of Electrical Engineering, National Chung Cheng University, Chia-Yi, Taiwan (e-mail: ieegwoyu@ccu.edu.tw).

Chen-Chih Chung is with Graduate Department of Electrical Engineering, National Chung Cheng University, Chia-Yi, Taiwan.

maximum and minimum functions. The researchers showed that the maximum-type piecewise Lyapunov functions cannot ensure stability in the control systems [19]; therefore, the stability conditions in this study were solved with minimum-type piecewise Lyapunov functions. However, the design of the controller of these systems is still limited to status feedback control. When the system adopts state feedback control for design, if the entire state of the system cannot be fully obtained, the design of an additional state estimator is required. This will increase the design complexity as well as decrease the reliability of the control system; hence, output feedback control is an ideal choice to solve this problem.

During networked control, data is usually transmitted in network packages. When the plant unpacks and decodes the data packages received from the controller, this requires time and thus also causes a delay [20-24]. Furthermore, a system's stability may be affected by external disturbances and model uncertainty in real-world situations [25, 26]. However, although some researchers have studied how to design polynomial fuzzy NCS [27], the robustness of these systems has not been evaluated, [28-30] considering that external disturbances [31-33] and model uncertainty account for external disturbances and model uncertainty [34-37]. Compared with a traditional polynomial fuzzy control system, polynomial fuzzy NCS is more resistant to external disturbances and mode uncertainty and provides better control performance. But these methods are all implemented based on a single Lyapunov without using piecewise Lyapunov functions and also without considering the time delay caused by the plant. As mentioned previously, a novel piecewise polynomial fuzzy network time-delay control method that combines the novel modeling method, the minimum-type piecewise Lyapunov function method, and robust stability analysis was adopted in this study.

Currently, the networked system has been created to gain the desired results of the team by exchanging information among the agents via the network due to technological advancements in data sensing and communication. Multi-agent formations that work in synergy must be designed. To achieve the desired goal tracking, the common formation control method involves establishing control strategies for each agent. Moreover, nonlinear problems also arise in the formation control. Several scholars have presented T-S fuzzy control solutions to the nonlinear problem of forming a leader-follower [38-40]. Since only the leader agent information is required to represent the behavior of the network team under the leader-follower scheme, the design of the multi-agent networked system could be simplified [41-45]. This has become one of the most popular and well-known strategies for solving the synchronization problem of networked systems. In comparison with T-S fuzzy control, polynomial fuzzy control has a larger feasible space. However, polynomial fuzzy control has not been used in formation control. In this work, combining polynomial fuzzy and leader-follower scheme, the controlled multi-agents networked system was allowed to gradually converge to the desired attitude and reference path with a specific form while ensuring the performance of the system.

The number of robots used in automation engineering has increased significantly, as robots are less expensive than labor, can produce unattended throughout the day and reduce human errors. Lights-out manufacturing has become the future trend in the long run. Among them, the automated guided vehicle moves from one device to another, transporting materials and handling machine parts as the main part. Clearly, path tracking control plays a crucial role, so it is important to assess how the control path is tracked is extremely important for the operation of the unmanned factory. Additionally, a formation of multiple agents can perform difficult tasks at higher efficiency with multiple capabilities by collaborating.

On the basis of the above references, this thesis proposes a networked control system using PPLFs based on a novel fuzzy model and polynomial fuzzy logic. This method can separate the largest and smallest parts of the antecedent variables into two categories. As a result, we can reduce the number of fuzzy rules to two, indicating that it can decrease chip calculation time.

To summarize, this study makes the following contributions:

1. Four SOS-based stability conditions are proposed for a novel piecewise polynomial fuzzy NCS with disturbances and uncertainties. The anti-interference ability of Theorem 4 satisfied the performance index, which could be used to simultaneously resist external interference and tolerate model uncertainty.

2. The application of the theorem in computer simulation and experiments of quadrotors and mobile robots shows that the theorem can have applications other than path tracking control. Moreover, it can solve the problems of package dropout and time delays caused by the network.

3. This study proposes a novel output feedback piecewise polynomial fuzzy network control system, which reduces the number of stability theorem inequalities derived. Therefore, using the proposed methods has a larger feasible solution space and better performance than the existing ones.

4. The proposed modeling method can greatly reduce the number of fuzzy rules. Hence, there are fewer control rules inside the system microprocessor, which can decrease chip calculation time, and thus reduce system hardware costs.

5. Compared with the existing methods, the proposed methods modeled the system matrix as a real system delay to overcome the time delay feedback signal caused by the plant.

6. This thesis combines the polynomial fuzzy network control system with the leader-follower scheme. In the simulation result, the multi-agent networked system successfully achieves the expected form formation tracking with stable tracking performance.

II. Novel Output Feedback Piecewise Polynomial Fuzzy Networked Control Time-Delay Systems

A. Networked Control Systems

It is essential to pay attention to the problems encountered when the system is connected to the network before introducing the piecewise polynomial fuzzy networked control time-delay systems. Fig. 1 shows the representative framework of NCSs. The NCSs are composed of controllers, sensors, plants, and actuators.

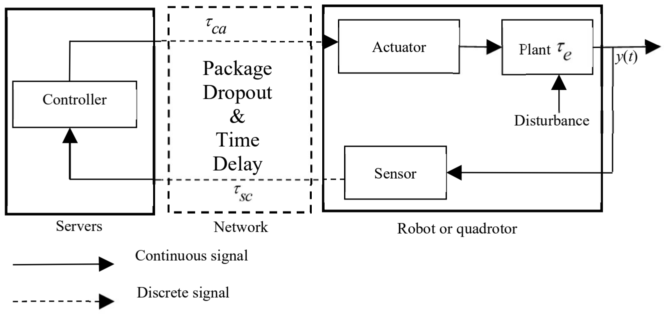

Fig. 1 The block diagram of NCSs.

Let t_k, t_{k+1}, …, t_{k+q} (k=0,1,2,…) indicate the sampling instants, $h_p=t_{k+1} - t_k$ means the sampling period, and $\tau_k, \tau_{k+1}, \cdots, \tau_{k+q}$ (q=1,2,…,$q_{\max}$) represent the total time delay caused by the network, and separated τ_k into τ_{sc} and τ_{ca}. The time delay τ_{sc} is caused by the transmitting data from the sensor to the controller via the network, and the time delay τ_{ca} is caused by the transmitting data from the controller to the actuator via the network, and set τ_e as the time delay caused by the plant, $\boldsymbol{v}$ is external disturbance.

Considering the delay and package dropout caused by the network, two parameters are often used to design the NCS controller. The first is the maximum allowable delay bound ρ, which is the maximum permissible control interval from the moment the sensors transmit the sampled data measured by the plant to the moment the actuators send the control signal. The second parameter is the maximum allowable transfer interval δ, which is a period of time; in other words, if a control signal is transmitted at a point in time $t_k + \tau_k$, then another should follow within the time interval $[t_k+\tau_k, t_k+\tau_k+\delta]$. Based on the two definitions above, $\lambda = \rho + \delta$ can be defined as the maximum allowable control interval to address both network-induced delay and package dropout problems simultaneously.

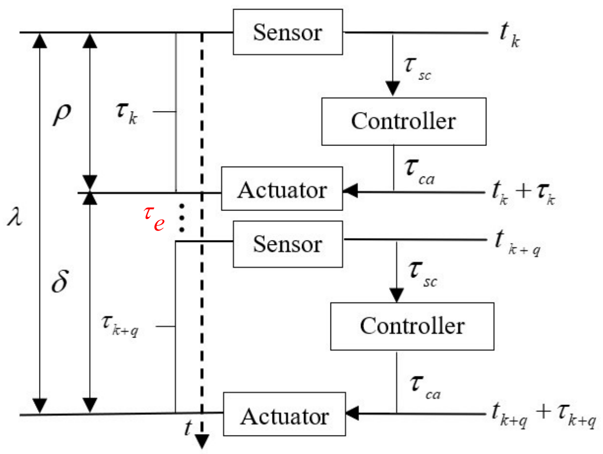

Fig. 2 Control signal time-sequence diagram.

For a given λ, inequality is assumed as follows:

$$t_{k+q} + \tau_{k+q} - t_k < \lambda \qquad q = 1, 2, \ldots, q_{\max} \tag{1}$$

where λ is an upper bound that ensures the closed-loop system maintains stability.

Moreover, the following is the definition of the number of data:

$$q_{\max} = INT\left(\frac{\lambda - \tau_{\max}}{h_p}\right) \tag{2}$$

where $\tau_{\max}$ is the maximum network-induced delay τ_k, and $INT(\cdot)$ denotes the integer parts of $(\cdot)$.

Thus, the maximum allowed package dropout rate $\varepsilon_{\max}$ can be obtained as follows:

$$\varepsilon_{\max} = \frac{q_{\max} - 1}{q_{\max}} \tag{3}$$

B. Minimum-Type Piecewise Polynomial Lyapunov Function

This section examines the definition and properties of the minimum-type PPLF. The minimum-type PPLF is obtained as follows:

$$\begin{aligned} &V_g(\boldsymbol{x}(t)) = \hat{\boldsymbol{x}}^T(\boldsymbol{x}(t))\boldsymbol{P}_g(\tilde{\boldsymbol{x}})\hat{\boldsymbol{x}}(\boldsymbol{x}(t)), \quad \boldsymbol{P}_g(\tilde{\boldsymbol{x}}) > 0, \quad g \in \{1, 2, \ldots, N\} \\ &V_q(\boldsymbol{x}(t)) = \min_{1 \le g \le N}\{V_g(\boldsymbol{x}(t))\} \end{aligned} \tag{4}$$

where N denotes the number of PPLFs segments, and defines all $\boldsymbol{P}_g(\tilde{\boldsymbol{x}})$ as positive definite symmetric polynomial matrix. Since $V_q(\boldsymbol{x}(t))$ is the minimum of $V_g(\boldsymbol{x}(t))$, properties of the minimum-type PPLF are shown as follows:

$$\sum_{g=1}^{N} \lambda_r \hat{\boldsymbol{x}}^T(\boldsymbol{x}(t))\left(\boldsymbol{P}_g(\tilde{\boldsymbol{x}}) - \boldsymbol{P}_q(\tilde{\boldsymbol{x}})\right)\hat{\boldsymbol{x}}(\boldsymbol{x}(t)) \ge 0 \tag{5}$$

where $\lambda_g \ge 0$ are the relaxing parameters.

C. Novel Output Feedback Piecewise Polynomial Fuzzy Networked Control Time-Delay Systems

This section presents a closed-loop novel piecewise polynomial fuzzy networked control time-delay system, combining a novel polynomial fuzzy model with external disturbances and model uncertainties and a novel piecewise controller based on output feedback.

Model Rule i:

IF $z_1(t)$ is M_{i1} and...and $z_p(t)$ is M_{ip}

$$THEN \begin{cases} \dot{\boldsymbol{x}}(t) = [\boldsymbol{A}_i(\boldsymbol{x}(t)) + \Delta\boldsymbol{A}_i]\hat{\boldsymbol{x}}(\boldsymbol{x}(t)) + [\boldsymbol{B}_i(\boldsymbol{x}(t)) + \Delta\boldsymbol{B}_i]\boldsymbol{u}(t) \\ \qquad + \boldsymbol{D}_i(\boldsymbol{x}(t))\boldsymbol{v}(t) + \boldsymbol{T}_i\boldsymbol{x}(t-\tau_e)] \\ \boldsymbol{y}(t) = \boldsymbol{C}_i(\boldsymbol{x}(t))\hat{\boldsymbol{x}}(\boldsymbol{x}(t)), \qquad i = 1, 2 \end{cases} \tag{6}$$

where $z(t) = [z_1(t), z_2(t), ..., z_p(t)]$ are the antecedent variables, $M_{ij}(j = 1, 2, ..., p)$ denotes the fuzzy set, $\boldsymbol{x}(t) = [x_1(t), x_2(t), \ldots, x_n(t)]^T \in \Re^n$ means a state vector, $\hat{\boldsymbol{x}}(\boldsymbol{x}(t)) \in \Re^{n \times 1}$ indicate a column vector whose entries are all monomials in $\boldsymbol{x}(t)$. $\boldsymbol{u}(t) \in \Re^m$ denotes the controller input vector and $\boldsymbol{y}(t) \in \Re^q$ is output vector. $\boldsymbol{A}_i(\boldsymbol{x}(t)) \in \Re^{n \times N}$, $\boldsymbol{B}_i(\boldsymbol{x}(t)) \in \Re^{n \times m}$ and $\boldsymbol{D}_i(\boldsymbol{x}(t)) \in \Re^{n \times p}$ are polynomial matrices, $\boldsymbol{C}_i \in \Re^{q \times N}$ and $\boldsymbol{T}_i \in \Re^{\boldsymbol{n} \times \boldsymbol{n}}$ are constant matrices, $\boldsymbol{v}(t) \in \Re^p$ means the external disturbance. $\Delta\boldsymbol{A}_i$ and $\Delta\boldsymbol{B}_i$ indicate the norm-bounded uncertainties defined as follows:

$$[\Delta\boldsymbol{A}_i, \Delta\boldsymbol{B}_i] = \boldsymbol{JK}(t)[\boldsymbol{R}_{ai}, \boldsymbol{R}_{bi}] \tag{7}$$

where $\boldsymbol{J}$, $\boldsymbol{R}_{ai}$, and $\boldsymbol{R}_{bi}$ are constant matrices with corresponding dimension. is a time-varying matrices bounded by $\boldsymbol{K}^T(t)\boldsymbol{K}(t) \le \boldsymbol{I}$.

The defuzzification result of novel polynomial fuzzy NCSs can be indicated as

$$\begin{cases} \dot{\boldsymbol{x}}(t) = \sum_{i=1}^{2} \begin{bmatrix} s_i(\boldsymbol{z}(t))(\boldsymbol{A}_i(\boldsymbol{x}(t)) + \Delta\boldsymbol{A}_i)\hat{\boldsymbol{x}}(\boldsymbol{x}(t)) \\ +s_i'(\boldsymbol{z}(t))(\boldsymbol{B}_i(\boldsymbol{x}(t)) + \Delta\boldsymbol{B}_i)\boldsymbol{u}(t) \\ +s_i(\boldsymbol{z}(t))\boldsymbol{D}_i(\boldsymbol{x}(t))\boldsymbol{v}(t) + s_i(\boldsymbol{z}(t))\boldsymbol{T}_i\boldsymbol{x}(t-\tau_e) \end{bmatrix} \\ \boldsymbol{y}(t) = \sum_{i=1}^{2} s_i(\boldsymbol{z}(t))\boldsymbol{C}_i(\boldsymbol{x}(t))\hat{\boldsymbol{x}}(\boldsymbol{x}(t)) \end{cases} \tag{8}$$

Considering that the model rules depend on the network environment, to stabilize the closed-loop system, the next step is to design the controller based on output feedback. Therefore, the control rules are obtained as follows:

Control Rule i:

$IF\ z_1(t_k)$ is M_{i1}, and...and $z_p(t_k)$ *is* M_{ip}

$$THEN\quad \boldsymbol{u}(t) = \boldsymbol{F}_{ig}(\boldsymbol{x}(t))\boldsymbol{y}(t_k),\quad \text{for } i = 1,2;\ g \in 1,2,...,N; \tag{9}$$

$t \in \left[t_k + \tau_k, t_{k+q} + \tau_{k+q}\right)$

where $\boldsymbol{F}_{ig}(\boldsymbol{x}(t))$ is the novel piecewise polynomial fuzzy control gain matrix.

The defuzzification of the control rules is shown as follows:

$$\boldsymbol{u}(t) = \sum_{i=1}^{2} \frac{s_i(\boldsymbol{z}(t_k))}{s_i'(\boldsymbol{z}(t))} \boldsymbol{F}_{ig}(\mathbf{x}(t))\mathbf{C}_i(\boldsymbol{x}(t))\hat{\boldsymbol{x}}(\boldsymbol{x}(t_k)), \text{for } i = 1,2 \tag{10}$$

Since the matrix C included in the output of the feedback compensation will cause nonconvex stability conditions, we considered a non-singular transformation matrix $\boldsymbol{L} \in \Re^{N\times N}$, which is obtained as

$$\boldsymbol{L} = \left[\boldsymbol{C}^T\left(\boldsymbol{C}\boldsymbol{C}^T\right)^{-1} \quad ortc(\boldsymbol{C}^T)\right] \tag{11}$$

where $ortc(C^T)$ means the orthogonal complement of C^T.

The time derivative of $\hat{\boldsymbol{x}}(\boldsymbol{x})$ is denoted by

$$\dot{\hat{\boldsymbol{x}}}(\boldsymbol{x}) = \frac{\partial\hat{\boldsymbol{x}}(\boldsymbol{x})}{\partial\boldsymbol{x}}\frac{d\boldsymbol{x}}{dt} = \boldsymbol{E}(\boldsymbol{x})\dot{\boldsymbol{x}} \tag{12}$$

where $\boldsymbol{E}(\boldsymbol{x}) \in \Re^{N\times n}$ is a polynomial matrix whose (i,j)-th entry is defined as

$$\boldsymbol{E}(\boldsymbol{x}) = \frac{\partial\hat{\boldsymbol{x}}(\boldsymbol{x})}{\partial\boldsymbol{x}} \tag{14}$$

For attenuating the influence of external disturbances, the H_∞ performance index is defined as

$$\int_{t_0}^{\infty} \boldsymbol{y}^T\boldsymbol{y}dt \le \gamma^2 \int_{t_0}^{\infty} \boldsymbol{v}^T\boldsymbol{v}dt \tag{15}$$

where $\gamma > 0$ denotes attenuation level, and $t_0 \ge 0$ means initial instant.

Define $\boldsymbol{z} = \boldsymbol{L}^{-1}\hat{\boldsymbol{x}}(\boldsymbol{x}(t))$, $\boldsymbol{z}_\tau = \boldsymbol{L}^{-1}\boldsymbol{x}(t-\tau_e)$ and $\boldsymbol{z}_k = \boldsymbol{L}^{-1}\hat{\boldsymbol{x}}(\boldsymbol{x}(t_k))$. The transformed output feedback system (8) can be obtained as

$$\dot{\boldsymbol{z}} = \sum_{i=1}^{2}\sum_{j=1}^{2} s_i s_j^k \begin{Bmatrix} \left[\tilde{\boldsymbol{A}}_i(\boldsymbol{x}) + \Delta\tilde{\boldsymbol{A}}_i\right]\boldsymbol{z} + \left[\tilde{\boldsymbol{B}}_i(\boldsymbol{x}) + \Delta\tilde{\boldsymbol{B}}_i\right]\boldsymbol{F}_{jg}(\boldsymbol{x})\boldsymbol{C}_j\boldsymbol{L}\boldsymbol{z}_k \\ +\tilde{\boldsymbol{D}}_i(\boldsymbol{x})\boldsymbol{v} + \boldsymbol{T}_i\boldsymbol{z}_\tau \end{Bmatrix}$$

$$\boldsymbol{y} = \sum_{i=1}^{2} s_i\left[\boldsymbol{C}_i\boldsymbol{L}\boldsymbol{z}\right],\quad g \in \{1,2,\ldots,N\},\ \boldsymbol{t} \in \left[\boldsymbol{t}_k + \tau_k, \boldsymbol{t}_{k+q} + \tau_{k+q}\right) \tag{16}$$

where the matrices can be defined as

$$\tilde{\boldsymbol{A}}_i(\boldsymbol{x}) = \boldsymbol{L}^{-1}\boldsymbol{E}(\boldsymbol{x})\boldsymbol{A}_i(\boldsymbol{x})\boldsymbol{L},\ \tilde{\boldsymbol{B}}_i(\boldsymbol{x}) = \boldsymbol{L}^{-1}\boldsymbol{E}(\boldsymbol{x})\boldsymbol{B}_i(\boldsymbol{x}),$$

$$\Delta\tilde{\boldsymbol{A}}_i = \boldsymbol{L}^{-1}\boldsymbol{E}(\boldsymbol{x})\Delta\boldsymbol{A}_i(\boldsymbol{x})\boldsymbol{L}, \Delta\tilde{\boldsymbol{B}}_i = \boldsymbol{L}^{-1}\boldsymbol{E}(\boldsymbol{x})\Delta\boldsymbol{B}_i(\boldsymbol{x})$$

$$\tilde{\boldsymbol{D}}_i(\boldsymbol{x}) = \boldsymbol{L}^{-1}\boldsymbol{E}(\boldsymbol{x})\boldsymbol{D}_i(\boldsymbol{x})$$

D.System Description of Formation Control

Fig. 3. shows the structure of the leader-follower team tracking networked system. Since each follower is requested to track the leader's trajectories, a specific error tracking augmented system is constructed by combining the leader's networked system with the followers' networked system with their corresponding desired tracking path and state. To ensure the team tracking performance of the nonlinear multi-agent system, the polynomial fuzzy formation control system is proposed, which comprises a polynomial fuzzy controller and polynomial fuzzy model.

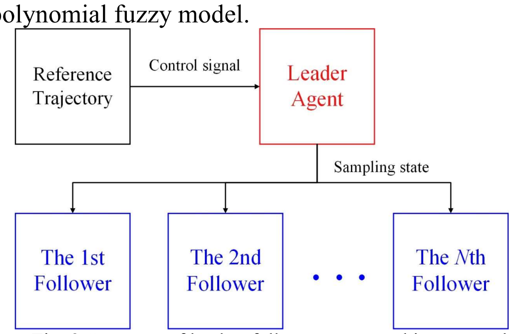

Fig. 3 Structure of leader–follower team tracking networked system.

The polynomial fuzzy formation model is defined as (17).

Model Rule i:

$IF\ z_1(t)$ is M_{i1} and...and $z_p(t)$ is M_{ip}

$$THEN\ \begin{cases} \dot{\boldsymbol{x}}_f(t) = \boldsymbol{A}_i(\boldsymbol{x}_f(t))\bar{\boldsymbol{x}}_f(\boldsymbol{x}_f(t)) + \boldsymbol{B}_i(\boldsymbol{x}_f(t))\boldsymbol{u}_f(t) \\ \boldsymbol{y}_f(t) = \boldsymbol{C}_i(\boldsymbol{x}_f(t))\bar{\boldsymbol{x}}_f(\boldsymbol{x}_f(t)),\quad i \in \{1,2,...,r\},\ f \in \{1,2,...,N\} \end{cases} \tag{17}$$

where $\boldsymbol{u}_f(t)$ represent the control input; N is the total number of agents and i is the fuzzy rule; $\boldsymbol{A}_i(\boldsymbol{x}_f(t)) \in \Re^{n\times N}$, $\boldsymbol{B}_i(\boldsymbol{x}_f(t)) \in \Re^{n\times m}$ are polynomial matrices; $\boldsymbol{C}_i \in \Re^{q\times N}$ is constant matrix.

Defined $\bar{\boldsymbol{x}}_f(\boldsymbol{x}_f(t))$ as a column vector whose entries are all monomials in $\boldsymbol{x}_f(t)$. The state vector is shown as

$$\bar{\boldsymbol{x}}_f(\boldsymbol{x}_f(t)) = \left(\boldsymbol{x}_f(t_k) - \boldsymbol{x}_r(t_k) - \boldsymbol{e}_{df}\right) \tag{18}$$

where $\boldsymbol{x}_f(t_k) - \boldsymbol{x}_r(t_k)$ as the tracking error between the fth agent to the virtual leader, and $\boldsymbol{e}_{df} = \left[e_{d1}^T,...,e_{dN}^T\right]$ denotes the desired formation between the fth agent and the virtual leader agent and e_{d1} equals to 0.

The defuzzification result of (17) is expressed as

$$\begin{cases} \dot{\boldsymbol{x}}_f(t) = \sum_{i=1}^{r} s_i(z_f(t))\left[A_i(\boldsymbol{x}_f(t))\bar{\boldsymbol{x}}_f(\boldsymbol{x}_f(t)) + \boldsymbol{B}_i(\boldsymbol{x}_f(t))\boldsymbol{u}_f(t)\right] \\ \boldsymbol{y}_f(t) = \sum_{i=1}^{r} s_i(z_f(t))C_i(\boldsymbol{x}_f(t))\bar{\boldsymbol{x}}_f(\boldsymbol{x}_f(t)),\ f \in \{1,2,...,N\} \end{cases} \tag{19}$$

The control rules are obtained as follows:

Control Rule i:

$IF\ z_1(t_k)$ is M_{i1}, and...and $z_p(t_k)$ *is* M_{ip}

$$THEN\ \boldsymbol{u}_f(t) = \boldsymbol{F}_{ig}(\boldsymbol{x}_f(t))\boldsymbol{y}_f(t_k), \tag{20}$$

$i \in \{1,2,...,r\}$, $f \in \{1,2,...,N\}$; $t \in \left[t_k + \tau_k, t_{k+q} + \tau_{k+q}\right)$

where $\boldsymbol{F}_{ig}(\boldsymbol{x}_f(t))$ is the polynomial fuzzy control gain matrix.

The defuzzification of the control rules are obtained as follows:

$$\boldsymbol{u}_f(t)=\sum_{i=1}^{r}\frac{s_i(z_f(t_k))}{s_i'(z_f(t))}\boldsymbol{F}_{ig}(\boldsymbol{x}_f(t))\boldsymbol{C}_i\bar{\boldsymbol{x}}_f(t_k),\ f\in\{1,2,\ldots,N\} \tag{21}$$

Define $z_f=\boldsymbol{L}^{-1}\bar{\boldsymbol{x}}_f(\boldsymbol{x}_f(t))$ and $z_{fk}=\boldsymbol{L}^{-1}\bar{\boldsymbol{x}}_f(\boldsymbol{x}_f(t_k))$. The transformed output feedback system (19) can be obtained as

$$\dot{z}_f=\sum_{i=1}^{r}\sum_{j=1}^{r}s_is_j\left[\bar{\boldsymbol{A}}_i(\boldsymbol{x}_f(t))z_f+\bar{\boldsymbol{B}}_i(\boldsymbol{x}_f(t))\boldsymbol{F}_{jg}\left(\boldsymbol{x}_f\right)\boldsymbol{C}_j\boldsymbol{L}\boldsymbol{z}_{fk}\right] \tag{22}$$
$$\boldsymbol{y}_f=\sum_{i=1}^{r}s_i\left[\boldsymbol{C}_i\boldsymbol{L}\boldsymbol{z}_f\right],\ f\in\{1,2,\ldots,N\},\ t\in\left[t_k+\tau_k,t_{k+q}+\tau_{k+q}\right)$$

where the matrices are obtained as

$$\bar{\boldsymbol{A}}_i(\boldsymbol{x})=\boldsymbol{L}^{-1}\boldsymbol{E}(\boldsymbol{x})\boldsymbol{A}_i(\boldsymbol{x})\boldsymbol{L},\bar{\boldsymbol{B}}_i(\boldsymbol{x})=\boldsymbol{L}^{-1}\boldsymbol{E}(\boldsymbol{x})\boldsymbol{B}_i(\boldsymbol{x})$$

III. Stability Analysis of Novel Piecewise Polynomial Fuzzy Networked Control Time-Delay Systems

An asymptotically stable closed-loop novel piecewise polynomial fuzzy time-delay control system (16) in a network-based environment is developed in this thesis by developing a method for designing the novel piecewise polynomial fuzzy controller (10). In order to simplify the notation, following will use $\boldsymbol{x}$, $\hat{\boldsymbol{x}}$, $\hat{\boldsymbol{x}}_k$, $\boldsymbol{A}_i(\boldsymbol{x})$, $\boldsymbol{B}_i(\boldsymbol{x})$, $\boldsymbol{F}_{jg}(\boldsymbol{x})$, s_i, s_j^k, and $\boldsymbol{y}$ to replace $\boldsymbol{x}(t)$, $\hat{\boldsymbol{x}}(\boldsymbol{x}(t))$, $\hat{\boldsymbol{x}}(\boldsymbol{x}(t_k))$, $\boldsymbol{A}_i(\boldsymbol{x}(t))$, $\boldsymbol{B}_i(\boldsymbol{x}(t))$, $\boldsymbol{F}_{jg}(\boldsymbol{x}(t))$, $s_i(\boldsymbol{z}(t))$, $s_j(\boldsymbol{z}(t_k))$, and $\boldsymbol{y}(t)$. In addition, several notations will be discussed. For instance, $\tilde{\boldsymbol{x}}=(x_{l_1},x_{l_2},\ldots,x_{l_n})$ is a chosen vector so as to $\boldsymbol{L}=\{l_1,l_2,\ldots,l_n\}$ indicates the row indices of $\boldsymbol{B}_i(\boldsymbol{x})$ whose corresponding row is equals to zero. $\boldsymbol{A}_i^l(\boldsymbol{x})$ represents the l_{th} row of $\boldsymbol{A}_i(\boldsymbol{x})$.

Theorem 1: The transformed closed-loop novel piecewise polynomial fuzzy networked control time-delay systems (20) is asymptotically stable if symmetric polynomial matrices $\boldsymbol{P}_g(\tilde{\boldsymbol{x}})$, $\boldsymbol{Q}_g(\boldsymbol{x})$, $\boldsymbol{R}_g(\boldsymbol{x})$ and polynomial matrices $\boldsymbol{H}_{jg}(\boldsymbol{x})(j=1,2)$, $\boldsymbol{X}_g(\tilde{\boldsymbol{x}})$, and $\boldsymbol{M}_{jg}(\boldsymbol{x})(j=1,2)$ with appropriate dimensions, let the SOS conditions satisfied with $\lambda>0,\ \gamma>0,\ \kappa>0$.

$$\boldsymbol{w}^T(\boldsymbol{P}_g(\tilde{\boldsymbol{x}})-\varepsilon_1(\boldsymbol{x})\boldsymbol{I})\boldsymbol{w}\text{ is SOS} \tag{23}$$
$$\boldsymbol{w}^T(\boldsymbol{Q}_g(\boldsymbol{x})-\varepsilon_2(\boldsymbol{x})\boldsymbol{I})\boldsymbol{w}\text{ is SOS} \tag{24}$$
$$\boldsymbol{w}^T(\boldsymbol{R}_g(\boldsymbol{x})-\varepsilon_3(\boldsymbol{x})\boldsymbol{I})\boldsymbol{w}\text{ is SOS} \tag{25}$$
$$-\boldsymbol{s}^T(\boldsymbol{\Phi}_{ijg}(\boldsymbol{x})-\varepsilon_4(\boldsymbol{x})\boldsymbol{I})\boldsymbol{s}\text{ is SOS},\quad \forall i\le j, \tag{26}$$

where $g\in 1,2,\ldots,N$ denote Nth PPLF, $\boldsymbol{w}$ and $\boldsymbol{s}$ are the matrices that are independent of $\boldsymbol{x}$ with appropriate dimensions. $\varepsilon_1(\boldsymbol{x})>0$, $\varepsilon_2(\boldsymbol{x})>0$, $\varepsilon_3(\boldsymbol{x})>0$ and $\varepsilon_4(\boldsymbol{x})>0$ are polynomial scalars.

The symmetric polynomial matrix $\boldsymbol{\Phi}_{ijg}(\boldsymbol{x})$ in (20) can be expressed as follows:

$$\boldsymbol{\Phi}_{ijg}(\boldsymbol{x})=\begin{bmatrix}
\boldsymbol{\Xi}_{11g} & \boldsymbol{\Xi}_{12g} & \boldsymbol{\Xi}_{13g} & 0 & -\tilde{D}_i(x(t)) & \lambda H_{1g}(x) & X_g^T(\tilde{x})L^TC_i^T(x) & -\tilde{J}\boldsymbol{X}_g(\tilde{x}) & \kappa X_g^T(\tilde{x})\tilde{R}_{ai}{}^T \\
* & \boldsymbol{\Xi}_{22g} & \boldsymbol{\Xi}_{23g} & 0 & -\tilde{D}_i(x(t)) & \lambda H_{2g}(x) & 0 & -\tilde{J}\boldsymbol{X}_g(\tilde{x}) & \kappa M_{jg}^T(\tilde{x})\tilde{R}_{bi}{}^T \\
* & * & \boldsymbol{\Xi}_{33g} & 0 & -\tilde{D}_i(x(t)) & \lambda H_{3g}(x) & 0 & -\tilde{J}\boldsymbol{X}_g(\tilde{x}) & 0 \\
* & * & * & \boldsymbol{\Xi}_{44g} & 0 & 0 & 0 & 0 & 0 \\
* & * & * & * & -\gamma^2\boldsymbol{I} & 0 & 0 & 0 & 0 \\
* & * & * & * & * & -\lambda Q_g(x) & 0 & 0 & 0 \\
* & * & * & * & * & * & -\boldsymbol{I} & 0 & 0 \\
* & * & * & * & * & * & * & -\kappa I & 0 \\
* & * & * & * & * & * & * & * & -\kappa I
\end{bmatrix} \tag{27}$$

where $*$ means the transposed matrix at the symmetrical position,

$$\boldsymbol{\Xi}_{11g}=\sum_{l\in L}\frac{\partial\boldsymbol{P}_g}{\partial\boldsymbol{x}_l}(\tilde{\boldsymbol{x}})\tilde{\boldsymbol{A}}_i^l(\boldsymbol{x})\hat{\boldsymbol{x}}+\boldsymbol{H}_{1g}(\boldsymbol{x})+\boldsymbol{H}_{1g}^T(\boldsymbol{x})-\tilde{\boldsymbol{A}}_i(\boldsymbol{x})\boldsymbol{X}_g(\tilde{\boldsymbol{x}})$$
$$-\boldsymbol{X}_g^T(\tilde{\boldsymbol{x}})\tilde{\boldsymbol{A}}_i^T(\boldsymbol{x})+\sum_{q=1}^{N}\lambda_q\boldsymbol{L}^T\left[\boldsymbol{P}_q(\tilde{\boldsymbol{x}})-\boldsymbol{P}_g(\tilde{\boldsymbol{x}})\right]\boldsymbol{L}$$
$$\boldsymbol{\Xi}_{12g}=\boldsymbol{H}_{2g}^T(\boldsymbol{x})-\boldsymbol{H}_{1g}(\boldsymbol{x})-\tilde{\boldsymbol{B}}_i(\boldsymbol{x})\boldsymbol{M}_{jg}(\boldsymbol{x})-\boldsymbol{X}_g^T(\tilde{\boldsymbol{x}})\tilde{\boldsymbol{A}}_i^T(\boldsymbol{x})$$
$$\boldsymbol{\Xi}_{13g}=\boldsymbol{P}_g(\tilde{\boldsymbol{x}})+\boldsymbol{H}_{3g}^T(\boldsymbol{x})+\boldsymbol{X}_g(\tilde{\boldsymbol{x}})-\boldsymbol{X}_g^T(\tilde{\boldsymbol{x}})\tilde{\boldsymbol{A}}_i^T(\boldsymbol{x})$$
$$\boldsymbol{\Xi}_{22g}=-\boldsymbol{H}_{2g}(\boldsymbol{x})-\boldsymbol{H}_{2g}^T(\boldsymbol{x})-\tilde{\boldsymbol{B}}_i(\boldsymbol{x})\boldsymbol{M}_{jg}(\boldsymbol{x})-\boldsymbol{M}_{jg}^T(\boldsymbol{x})\tilde{\boldsymbol{B}}_i^T(\boldsymbol{x})$$
$$\boldsymbol{\Xi}_{23g}=\boldsymbol{X}_g(\tilde{\boldsymbol{x}})-\boldsymbol{H}_{3g}^T(\boldsymbol{x})-\boldsymbol{M}_{jg}^T(\boldsymbol{x})\tilde{\boldsymbol{B}}_i^T(\boldsymbol{x})$$
$$\boldsymbol{\Xi}_{33g}=\lambda\boldsymbol{Q}_g(\boldsymbol{x})+\boldsymbol{X}_g(\tilde{\boldsymbol{x}})+\boldsymbol{X}_g^T(\tilde{\boldsymbol{x}})$$
$$\boldsymbol{\Xi}_{44g}=\boldsymbol{R}_g(\boldsymbol{x})$$
$$\tilde{\boldsymbol{J}}=\boldsymbol{L}^{-1}\boldsymbol{J},\ \tilde{\boldsymbol{R}}_{ai}=\boldsymbol{R}_{ai}\boldsymbol{L},\ \tilde{\boldsymbol{R}}_{bi}=\boldsymbol{R}_{bi}$$

Proof: Please see the appendix1.

Remark: Without considering the time-delay matrix $\boldsymbol{R}_g(\boldsymbol{x})$, the novel piecewise polynomial fuzzy networked control time-delay system can be reduced to the novel piecewise polynomial fuzzy networked control system. Therefore, the conditions of the novel piecewise polynomial fuzzy networked control systems with external disturbances and model uncertainties are special cases of the novel piecewise polynomial fuzzy networked control time-delay systems with model uncertainties and external disturbances.

Theorem 2: In this section, we describe the stability conditions for piecewise polynomial fuzzy networked control systems derived from the SOS. This study proposes a method for designing a switching polynomial fuzzy controller (21) so that a closed-loop polynomial fuzzy system (22) can be globally stable in a networked environment. The transformed output feedback system base on the transformed output feedback system can be represented as follows:

$$\boldsymbol{w}^T\left(\boldsymbol{P}_g\left(\tilde{\boldsymbol{x}}_f\right)-\varepsilon_1\left(\boldsymbol{x}_f\right)\boldsymbol{I}\right)\boldsymbol{w}\text{ is SOS} \tag{28}$$
$$\boldsymbol{w}^T\left(\boldsymbol{Q}_g\left(\boldsymbol{x}_f\right)-\varepsilon_2\left(\boldsymbol{x}_f\right)\boldsymbol{I}\right)\boldsymbol{w}\text{ is SOS} \tag{29}$$
$$-\boldsymbol{s}^T\left(\boldsymbol{\Phi}_{ijg}\left(\boldsymbol{x}_f\right)+\varepsilon_3\left(\boldsymbol{x}_f\right)\boldsymbol{I}\right)\boldsymbol{s}\text{ is SOS},\quad\forall i\le j, \tag{30}$$

where $g\in 1,2,\ldots,N$ denote Nth PPLF, $\boldsymbol{w}$ and $\boldsymbol{s}$ are the matrices that are independent of $\boldsymbol{x}$ with appropriate dimensions. $\varepsilon_1(\boldsymbol{x})>0$, $\varepsilon_2(\boldsymbol{x})>0$ and $\varepsilon_3(\boldsymbol{x})>0$ are polynomial scalars.

The symmetric polynomial matrix $\boldsymbol{\Phi}_{ijg}(\boldsymbol{x}_f)$ in (30) can be expressed as follows:

$$\boldsymbol{\Phi}_{ijg}(\boldsymbol{x}_f)=\begin{bmatrix}
\boldsymbol{\Xi}_{11g} & \boldsymbol{\Xi}_{12g} & \boldsymbol{\Xi}_{13g} & -\tilde{D}_i(x_f) & \lambda H_{1g}(x_f) & X_g^T(\tilde{x}_f)L^TC_i^T(x_f) & -\tilde{J}\boldsymbol{X}_g(\tilde{x}_f) & \kappa X_g^T(\tilde{x}_f)\tilde{R}_{ai}{}^T \\
* & \boldsymbol{\Xi}_{22g} & \boldsymbol{\Xi}_{23g} & -\tilde{D}_i(x_f) & \lambda H_{2g}(x_f) & 0 & -\tilde{J}\boldsymbol{X}_g(\tilde{x}_f) & \kappa M_{jg}^T(\tilde{x}_f)\tilde{R}_{bi}{}^T \\
* & * & \boldsymbol{\Xi}_{33g} & -\tilde{D}_i(x_f) & \lambda H_{3g}(x_f) & 0 & -\tilde{J}\boldsymbol{X}_g(\tilde{x}_f) & 0 \\
* & * & * & -\gamma^2\boldsymbol{I} & 0 & 0 & 0 & 0 \\
* & * & * & * & -\lambda Q_g(x_f) & 0 & 0 & 0 \\
* & * & * & * & * & -\boldsymbol{I} & 0 & 0 \\
* & * & * & * & * & * & -\kappa I & 0 \\
* & * & * & * & * & * & * & -\kappa I
\end{bmatrix} \tag{31}$$

where $*$ means the transposed matrix at the symmetrical position,

$$\boldsymbol{\Xi}_{11g}=\sum_{l\in L}\frac{\partial\boldsymbol{P}_g}{\partial\boldsymbol{x}_l}\left(\tilde{\boldsymbol{x}}_f\right)\bar{\boldsymbol{A}}_i^l\left(\boldsymbol{x}_f\right)\bar{\boldsymbol{x}}+\boldsymbol{H}_{1g}\left(\boldsymbol{x}_f\right)+\boldsymbol{H}_{1g}^T\left(\boldsymbol{x}_f\right)-\bar{\boldsymbol{A}}_i\left(\boldsymbol{x}_f\right)\boldsymbol{X}_g\left(\tilde{\boldsymbol{x}}_f\right)$$
$$-\boldsymbol{X}_g^T\left(\tilde{\boldsymbol{x}}_f\right)\bar{\boldsymbol{A}}_i^T\left(\boldsymbol{x}_f\right)+\sum_{q=1}^{N}\lambda_q\boldsymbol{L}^T\left[\boldsymbol{P}_q\left(\tilde{\boldsymbol{x}}_f\right)-\boldsymbol{P}_g\left(\tilde{\boldsymbol{x}}_f\right)\right]\boldsymbol{L}$$
$$\boldsymbol{\Xi}_{12g}=\boldsymbol{H}_{2g}^T\left(\boldsymbol{x}_f\right)-\boldsymbol{H}_{1g}\left(\boldsymbol{x}_f\right)-\bar{\boldsymbol{B}}_i\left(\boldsymbol{x}_f\right)\boldsymbol{M}_{jg}\left(\boldsymbol{x}_f\right)-\boldsymbol{X}_g^T\left(\tilde{\boldsymbol{x}}_f\right)\bar{\boldsymbol{A}}_i^T\left(\boldsymbol{x}_f\right)$$
$$\boldsymbol{\Xi}_{13g}=\boldsymbol{P}_g\left(\tilde{\boldsymbol{x}}_f\right)+\boldsymbol{H}_{3g}^T\left(\boldsymbol{x}_f\right)+\boldsymbol{X}_g\left(\tilde{\boldsymbol{x}}_f\right)-\boldsymbol{X}_g^T\left(\tilde{\boldsymbol{x}}_f\right)\bar{\boldsymbol{A}}_i^T\left(\boldsymbol{x}_f\right)$$

$$\boldsymbol{\Xi}_{22g}=-\boldsymbol{H}_{2g}\left(\boldsymbol{x}_f\right)-\boldsymbol{H}_{2g}^T\left(\boldsymbol{x}_f\right)-\overline{\boldsymbol{B}}_i\left(\boldsymbol{x}_f\right)\boldsymbol{M}_{jg}\left(\boldsymbol{x}_f\right)-\boldsymbol{M}_{jg}^T\left(\boldsymbol{x}_f\right)\overline{\boldsymbol{B}}_i^T\left(\boldsymbol{x}_f\right)$$
$$\boldsymbol{\Xi}_{23g}=\boldsymbol{X}_g\left(\tilde{\boldsymbol{x}}_f\right)-\boldsymbol{H}_{3g}^T\left(\boldsymbol{x}_f\right)-\boldsymbol{M}_{jg}^T\left(\boldsymbol{x}_f\right)\overline{\boldsymbol{B}}_i^T\left(\boldsymbol{x}_f\right)$$
$$\boldsymbol{\Xi}_{33g}=\lambda\boldsymbol{Q}_g\left(\boldsymbol{x}_f\right)+\boldsymbol{X}_g\left(\tilde{\boldsymbol{x}}_f\right)+\boldsymbol{X}_g^T\left(\tilde{\boldsymbol{x}}_f\right)$$

Proof: Please see the appendix2.

IV. Novel Piecewise Polynomial Fuzzy Networked Control Time-Delay Systems of a Mobile Robot and a Quadrotor

A. Kinematic Model of a Mobile Robot

In this section, v means the linear velocity of the mobile robot, and its direction points to the heading direction. ω means the angular velocity of the mobile robot, and its direction is the x-axis points counterclockwise to the heading direction. Based on the definition of the linear velocity and the angular velocity, the kinematic model is obtained as

$$\begin{bmatrix}\dot{x}\\ \dot{y}\\ \dot{\theta}\end{bmatrix}=\begin{bmatrix}v\cos\theta\\ v\sin\theta\\ w\end{bmatrix} \tag{32}$$

The posture error dynamic equation can be shown as follows:

$$\begin{bmatrix}\dot{e}_x\\ \dot{e}_y\\ \dot{e}_\theta\end{bmatrix}=\begin{bmatrix}\cos e_\theta & 0\\ \sin e_\theta & 0\\ 0 & 1\end{bmatrix}\begin{bmatrix}v_r\\ w_r\end{bmatrix}+\begin{bmatrix}-1 & e_y\\ 0 & -e_x\\ 0 & -1\end{bmatrix}\boldsymbol{u}+\begin{bmatrix}0 & 0.1 & 0\\ -0.1 & 0 & 0\\ 0 & 0 & 0.1\end{bmatrix}\begin{bmatrix}e_{x\tau}\\ e_{y\tau}\\ e_{\theta\tau}\end{bmatrix} \tag{33}$$

B. Novel Piecewise Polynomial Fuzzy Time-Delay Networked Modeling of a Mobile Robot

The input vector of the mobile robot includes the feedback control vector u_B and the feed-forward input control vector u_F. It can be written as follows:

$$\boldsymbol{u}=\boldsymbol{u}_B+\boldsymbol{u}_F \tag{34}$$

where

$\boldsymbol{u}_B=\begin{bmatrix}v_a & w_a\end{bmatrix}^T$, $\boldsymbol{u}_F=\begin{bmatrix}v_r\cos e_\theta & w_r\end{bmatrix}^T$.

The posture error dynamic equation can be shown as follows:

$$\begin{bmatrix}\dot{e}_x\\ \dot{e}_y\\ \dot{e}_\theta\end{bmatrix}=\begin{bmatrix}0 & w_r & 0\\ -w_r & 0 & v_r\dfrac{\sin e_\theta}{e_\theta}\\ 0 & 0 & 0\end{bmatrix}\begin{bmatrix}e_x\\ e_y\\ e_\theta\end{bmatrix}+\begin{bmatrix}-1 & e_y\\ 0 & -e_x\\ 0 & -1\end{bmatrix}\begin{bmatrix}v_a\\ w_a\end{bmatrix}+\begin{bmatrix}0 & 0.1 & 0\\ -0.1 & 0 & 0\\ 0 & 0 & 0.1\end{bmatrix}\begin{bmatrix}e_{x\tau}\\ e_{y\tau}\\ e_{\theta\tau}\end{bmatrix} \tag{35}$$

Since ω_r and v_r are nonlinear terms, define w_r as the antecedent variable $z_1(t)$ and v_r the antecedent variable $z_2(t)$.

C. Kinematic Model of a Quadrotor

The position of a moving quadrotor defined as $x(t)$, $y(t)$, and $z(t)$ are linear functions. Furthermore, the attitude of a moving quadrotor is determined on the basis of three Euler angles. $\phi(t)$ represents the roll angle, $\theta(t)$ represents the pitch angle, and $\psi(t)$ represents the yaw angle. By ignoring the drag coefficient and assuming the architecture of the quadrotor kinematic model is symmetric, the following equation can be derived:

$$\ddot{x}=(\sin\phi\sin\psi+\cos\phi\sin\theta\cos\psi)\frac{u_{alt}}{M} \tag{36}$$

$$\ddot{y}=(\cos\phi\sin\theta\sin\psi-\sin\phi\cos\psi)\frac{u_{alt}}{M} \tag{37}$$

$$\ddot{z}=(\cos\phi\cos\theta)\frac{u_{alt}}{M}-g \tag{38}$$

$$\ddot{\phi}=\frac{J_y-J_z}{J_x}\dot{\theta}\dot{\psi}+\frac{1}{J_x}\tau_x \tag{39}$$

$$\ddot{\theta}=\frac{J_z-J_x}{J_y}\dot{\phi}\dot{\psi}+\frac{1}{J_y}\tau_y \tag{40}$$

$$\ddot{\psi}=\frac{J_x-J_y}{J_z}\dot{\phi}\dot{\theta}+\frac{1}{J_z}\tau_z \tag{41}$$

where the mass of the quadrotor is M. g represents the acceleration of gravity of the earth. The moments of inertia for each axis are defined as J_x, J_y, and J_z. u_{alt} is the lift of the quadrotor. τ_x, τ_y, and τ_z represents the torques of the x-axis, y-axis, and z-axis, respectively.

The following formula can be used to express the relationships between quadrotor control and propeller rotation speeds:

$$u_{alt}=b(\omega_1^2+\omega_2^2+\omega_3^2+\omega_4^2) \tag{42}$$

$$\tau_x=lb(-\omega_2^2+\omega_4^2) \tag{43}$$

$$\tau_y=lb(-\omega_1^2+\omega_3^2) \tag{44}$$

$$\tau_z=d(-\omega_1^2+\omega_2^2-\omega_3^2+\omega_4^2) \tag{45}$$

where b represents the lift coefficient; l means the distance between each propeller to the center of the mass. d means the drag coefficient of the propeller. $\omega 1$, $\omega 2$, $\omega 3$, and $\omega 4$ indicate the rotational speeds of the four propellers of the quadrotor, respectively.

D. Novel Piecewise Polynomial Fuzzy Time-Delay Networked Modeling of a Quadrotor

In this section, a novel polynomial fuzzy model of a quadrotor is introduced. The fuzzy rules were reduced from six to two, decreasing the calculation time for the microprocessor. In this section, we discuss three types of controllers, including altitude controller, position controller, and attitude controller.

(a) Altitude Subsystem

The reference altitude of the quadrotor is defined as $z_r(t)$, the altitude variation due to time delay is defined as z_τ, and the state altitude error can be defined as follows:

$$x_{alt}=\begin{bmatrix}z-z_v & \dot{z}-\dot{z}_v\end{bmatrix}^T \tag{46}$$

The altitude error model can be obtained:

$$\dot{\boldsymbol{x}}_{alt}=\boldsymbol{A}_{alt}\boldsymbol{x}_{alt}+\boldsymbol{B}_{alt}\boldsymbol{u}_{alt}+\boldsymbol{B}_{alt}\boldsymbol{f}_{alt} \tag{47}$$

where $\boldsymbol{A}_{alt}=\begin{bmatrix}0 & 1\\ 0 & 0\end{bmatrix}$, $\boldsymbol{B}_{alt}=\begin{bmatrix}0\\ \dfrac{\cos\phi\cos\theta}{M}\end{bmatrix}$, $f_{alt}=\dfrac{M}{\cos\phi\cos\theta}\times(-g-\ddot{z}_v-0.1\dot{z}_\tau)$.

Since $\dfrac{\cos\phi\cos\theta}{M}$ is a nonlinear term, define $z_1=\dfrac{\cos\phi\cos\theta}{M}$ as the antecedent variable.

(b) Position Subsystem

$x_v(t)$ and $y_v(t)$ are defined as the reference position of the quadrotor, $x_\tau(t)$ and $y_\tau(t)$ are defined as the position variation due to the time delay of the quadrotor, and the state position error can be defined as follows:

$$x_{pos}=\begin{bmatrix}x-x_v & y-y_v & \dot{x}-\dot{x}_v & \dot{y}-\dot{y}_v & \int x-x_v & \int y-y_v\end{bmatrix}^T \tag{48}$$

The position error model can be obtained:

$$\dot{\boldsymbol{x}}_{pos}=\boldsymbol{A}_{pos}\boldsymbol{x}_{pos}+\boldsymbol{B}_{pos}\boldsymbol{u}_{pos}+\boldsymbol{B}_{pos}\boldsymbol{f}_{pos} \tag{49}$$

where

$$\boldsymbol{A}_{pos}=\begin{bmatrix}0&0&1&0&0&0\\0&0&0&1&0&0\\0&0&0&0&0&0\\0&0&0&0&0&0\\1&0&0&0&0&0\\0&1&0&0&0&0\end{bmatrix},\ \boldsymbol{B}_{pos}=\begin{bmatrix}0&0\\0&0\\\frac{u_{alt}}{M}&0\\0&\frac{u_{alt}}{M}\\0&0\\0&0\end{bmatrix},\ \boldsymbol{f}_{pos}=\begin{bmatrix}-\frac{M}{u_{alt}}(\ddot{x}_v+0.1\dot{x}_\tau)\\-\frac{M}{u_{alt}}(\ddot{y}_v-0.1\dot{y}_\tau)\end{bmatrix},$$

$$\boldsymbol{u}_{pos}=\begin{bmatrix}u_{pos,1}\\u_{pos,2}\end{bmatrix}=\begin{bmatrix}\cos\varphi\sin\theta\cos\psi+\sin\varphi\sin\psi\\\cos\varphi\sin\theta\sin\psi-\sin\varphi\cos\psi\end{bmatrix}$$

Since $\frac{u_{alt}}{M}$ is a nonlinear term, define $z_2=\frac{u_{alt}}{M}$ being the premise variable.

(c)

(d) Attitude Subsystem

$\phi_v(t)$, $\theta_v(t)$, and $\psi_v(t)$ are defined as the reference attitude of the quadrotor, and $\phi_\tau(t)$, $\theta_\tau(t)$, and $\psi_\tau(t)$ are defined as the attitude variation due to the time delay of the quadrotor, and the state attitude error can be defined as follows:

$$\dot{\boldsymbol{x}}_{\text{att}}=\boldsymbol{A}_{\text{att}}\boldsymbol{x}_{\text{att}}+\boldsymbol{B}_{\text{att}}\boldsymbol{u}_{\text{att}}+\boldsymbol{F}_{\text{att}} \tag{51}$$

where

$$\boldsymbol{A}_{att}=\begin{bmatrix}0&0&0&1&0&0\\0&0&0&0&1&0\\0&0&0&0&0&1\\0&0&0&0&0&\frac{J_y-J_z}{J_x}\dot{\theta}\\0&0&0&\frac{J_z-J_x}{J_y}\dot{\psi}&0&0\\0&0&0&0&\frac{J_x-J_y}{J_z}\dot{\phi}&0\end{bmatrix},\ \boldsymbol{B}_{att}=\begin{bmatrix}0&0&0\\0&0&0\\0&0&0\\\frac{1}{J_x}&0&0\\0&\frac{1}{J_y}&0\\0&0&\frac{1}{J_z}\end{bmatrix},\ \boldsymbol{u}_{att}=\begin{bmatrix}\tau_x\\\tau_y\\\tau_z\end{bmatrix}$$

$$\boldsymbol{F}_{att}=\begin{bmatrix}a_1\dot{\theta}\dot{\psi}_v-J_x\ddot{\varphi}_v+0.1a_1\dot{\theta}\dot{\psi}_\tau\\a_2\dot{\psi}\dot{\varphi}_v-J_y\ddot{\theta}_v+0.1a_2\dot{\psi}\dot{\varphi}_\tau\\a_3\dot{\varphi}\dot{\theta}_v-J_z\ddot{\psi}_v+0.1a_3\dot{\varphi}\dot{\theta}_\tau\end{bmatrix}.$$

Since $\dot{\phi}$, $\dot{\theta}$, and $\dot{\psi}$ are nonlinear terms, define $z_3=\dot{\phi}$, $z_4=\dot{\theta}$, and $z_5=\dot{\psi}$ as the antecedent variables.

V. Results

(a) Package dropout

To prove that the negative impact of package dropout on NCSs and package dropout is stochastic, we set the package dropout rate $\zeta=50\%$ and the disturbance to occur at 20 to 21 s, with a pulse with an amplitude of 0.8. The time response of the system states and sampled input under package dropout and time delay conditions are shown in Fig. 4- Fig. 6. Since package dropout is a random event, the error time response graphs of x, y, and θ are presented in four simulations. The red line is a discrete signal, and the blue line is a continuous signal. Based on these, an apparent simulation diagram is provided that the proposed new piecewise polynomial fuzzy controller can still correctly track continuous signals when the network causes package dropout. This verifies that the proposed novel piecewise polynomial fuzzy controller can effectively control the network system while ensuring the stability of the system.

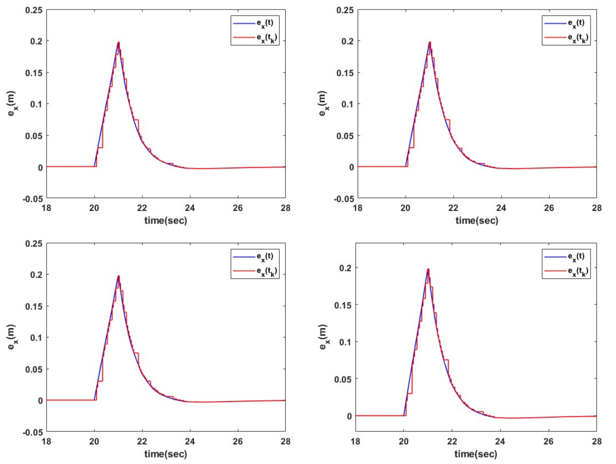

Fig. 4 Time responses of $e_x(t_k)$, $e_x(t)$.

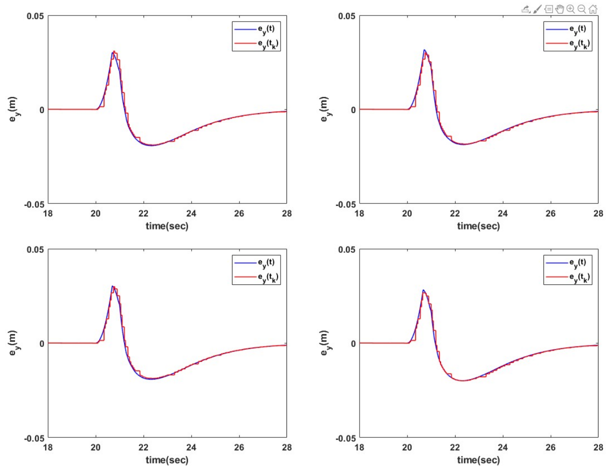

Fig. 5 Time responses of $e_y(t_k)$, $e_y(t)$.

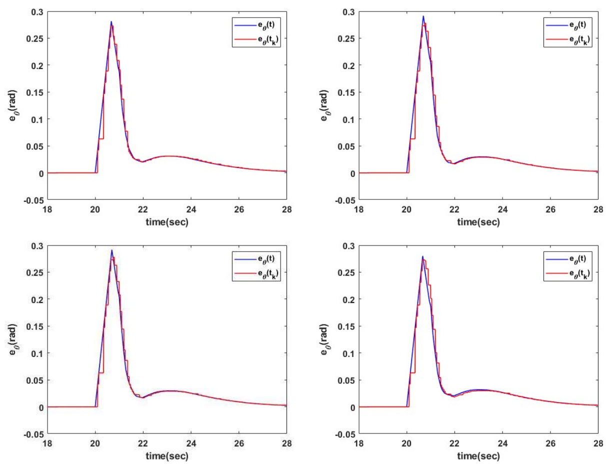

Fig. 6 Time responses of $e_\theta(t_k)$, $e_\theta(t)$.

The package dropout rate was set to $\zeta=50\%$ and the disturbance was set to occur at 20 to 21 s, with a pulse with an amplitude of 0.8. Since package dropout is a random event, the error time response of z, and ϕ are presented in four simulations, respectively, as shown in Fig. 7 and Fig. 8. Based on the following, the apparent simulation diagram is provided that the proposed new piecewise polynomial fuzzy controller can still correctly track continuous signals when the network causes package dropout. This verifies that the proposed novel piecewise polynomial fuzzy controller can effectively control the network system while ensuring the stability of the system.

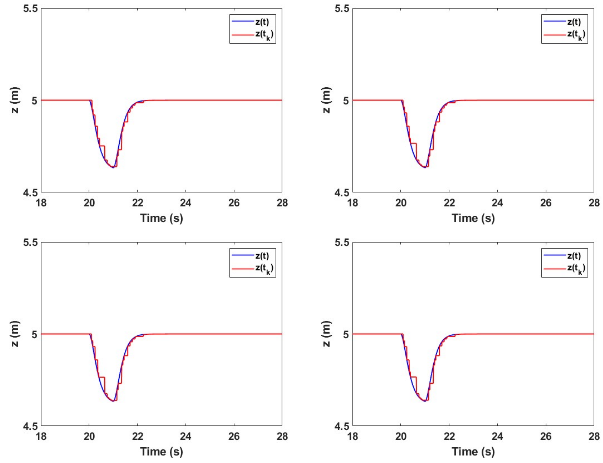

Fig. 7 Time responses of $z(t_k)$, $z(t)$.

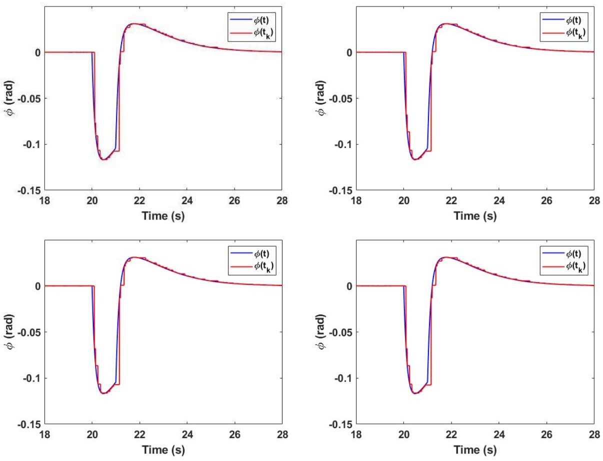

Fig. 8 Time responses of $\phi(t_k)$, $\phi(t)$.

(b) Feasible solution space

Fig. 9 shows the comparison of feasible spaces corresponding to different methods. The feasible solution space of novel polynomial fuzzy networked control time-delay systems is bigger than the existing novel polynomial fuzzy networked control time-delay systems.

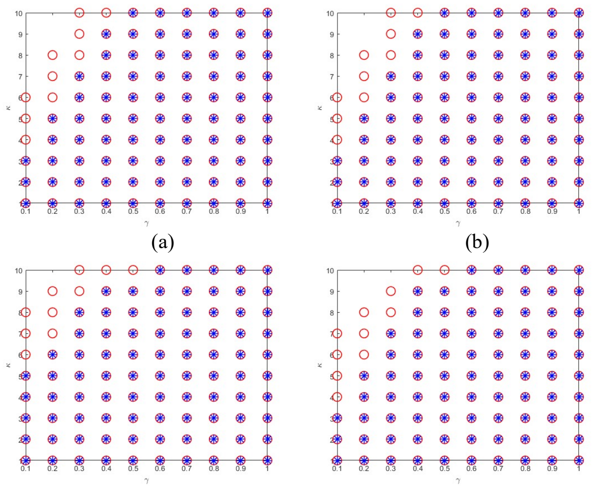

(a) (b) (c) (d)

Fig. 9 (a) Feasible solution space of control system for the mobile robot. (b) Feasible solution space of altitude subsystem for the quadrotor. (c) Feasible solution space of position subsystem for the quadrotor. (d) Feasible solution space of attitude subsystem for the quadrotor. (N=2)

A comparison of the proposed method with the existing method indicated an increase in both the number of fuzzy rules and stability conditions. It can be verified by computing time in Table 1.

Table 1. The comparison of different approach (*N*=2).

Methods	**Fuzzy rules**	**Stability conditions**	**Average of the CPU computation time**
Novel SOS	2	12	14.5968 μs
Existing SOS	4	266	28.6357 μs

Simulation Results

This section describes the simulations of the mobile robots and quadrotors to simulate the theorems. To compare the control performance of the proposed methods, the integrated square error performance index is defined as follows to compare the performance of the proposed method:

$$\text{ISE} = \int_0^{t_f} \boldsymbol{e}^T \boldsymbol{e} dt \tag{56}$$

The simulation parameters of the quadrotor are shown in Table 1. Thus, the altitude output matrix $\boldsymbol{C}_{alt,i}$, position output matrix $\boldsymbol{C}_{pos,i}$, and attitude output matrix $\boldsymbol{C}_{att,i}$ are expressed as follows:

$$C_{alt,i} = [1 \quad 0],\ C_{pos,i} = C_{att,i} = [1 \quad 1 \quad 0 \quad 0 \quad 0 \quad 0]$$

Table 2. The parameters of the quadrotor.

Notation	Value	Unit	Notation	Value	Unit
g	9.81	m/s^2	d	1.1×10^{-6}	N·m·s^2
M	2.4	kg	J_x	8.1×10^{-3}	N·m·s^2
l	0.275	m	J_y	8.1×10^{-3}	N·m·s^2
b	54.2×10^{-6}	N·s^2	J_z	14.2×10^{-3}	N·m·s^2
R	0.175	m			

In addition, set the sampling period $h_p = 0.05$, $\lambda = 0.2$, $\tau_e = 1$, and network-induced delay time $\tau_k = 0.045\times rand$, where $rand$ means a random value between 0 and 1. Based on (2), the interval of maximal allowable package dropout can be calculated as follows:

$$\varepsilon_{\max} = INT\left(\frac{0.2-0.045\times1}{0.05}\right) = 3 \tag{57}$$

It means that the maximal allowable package dropout rate is equal to 66.7%.

(a) Mobile Robot

With the initial value $x(0) = [0 \quad 0]^T$ as the coordinate of the robot and 0.5 as the package dropout rate, the reference linear velocity and angular velocity are $v_r = 0.5(\text{m/s})$ and $\omega_r = -\sin(\frac{2\pi t}{15.118})(\text{rad/s})$, respectively. Then, the mobile robot will start trajectory tracking of infinity.

The error comparison is shown in Fig. 10. The error of the proposed method is shown in red, while the error of the existing method is shown in blue. The segment of the Lyapunov function is equal to 2. In the figure, the red line shows a faster response speed at the beginning than the blue line does, and the magnitude of oscillation is smaller. Fig. 11 shows the tracking trajectory of the mobile robot in the X-Y plane. The black line represents the desired trajectory, the red line means the proposed method tracking trajectory, and the blue line means the existing method tracking trajectory. According to the figure, the red line demonstrates better tracking performance than the blue line.

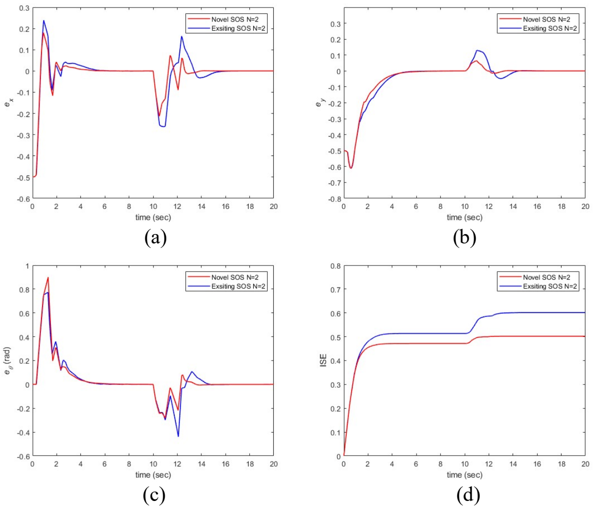

Fig. 10 (a) Time responses of $e_x(t)$. (b) Time responses of $e_y(t)$. (c) Time responses of $e_\theta(t)$. (d) Time responses of ISE.

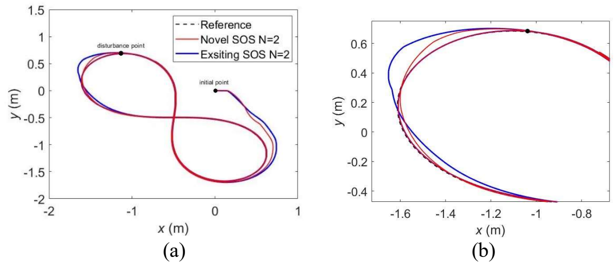

Fig. 11 (a) The trajectory of mobile robot. (b) The detail of trajectory of mobile robot.

Next, based on theorem2 with the initial value $\boldsymbol{x}_1(0)=[-0.25 \quad -0.25]^T$ as the coordinate of the leader, $\boldsymbol{x}_2(0)=[-0.5 \quad -0.25]^T$ and $e_2(0)=[-0.2 \quad -0.2]^T$ as the coordinate and the desired formation of follower 1, $\boldsymbol{x}_3(0)=[0 \quad -0.15]^T$ and $e_3(0)=[-0.2 \quad 0.2]^T$ as the coordinate and the desired formation of follower 2, and 0.5 as the package dropout rate, the error comparison used the proposed method is shown in Fig. 12. The error of the leader is shown in red, while the error of the follower 1 is shown in blue, while the error of the follower 2 is shown in green. In the figure, the blue line shows the smallest magnitude of oscillation at the beginning than the other lines do. It is because follower 1 was set as the closest to the desired form. Fig. 13 shows the tracking trajectory of mobile robots in the X-Y plane. The red line is the tracking trajectory of the leader, the blue line represents the tracking trajectory of follower 1, and the green line represents the tracking trajectory of follower 2. The figure shows that followers can effectively form a triangle formation with the leader.

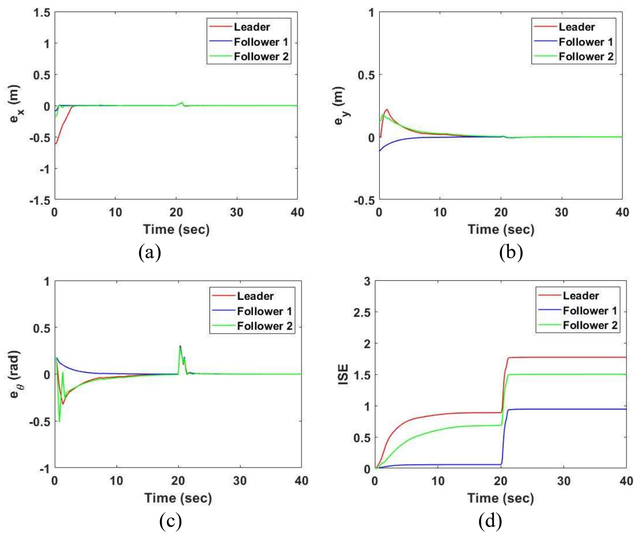

Fig .12 (a) Time responses of $e_x(t)$. (b) Time responses of $e_y(t)$. (c) Time responses of $e_\theta(t)$. (d) Time responses of ISE.

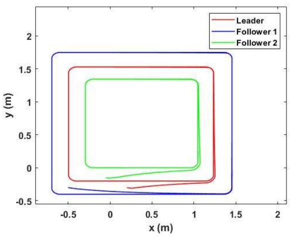

Fig .13 The trajectory of mobile robot.

(b) Quadrotor

Furthermore, the initial conditions of the quadrotor are given as $x=0$ (m), $y=0$ (m), $z=0$ (m), $\phi=0$(deg), $\theta=0$(deg), and $\psi=0$(deg). Setting the packet dropout rate as 0.5, the reference conditions of the quadrotor are defined as follows:

$$v_r=0.5\ \text{(m/s)},\ \omega_r=-\sin\left(\frac{2\pi t}{15.118}\right)\text{(rad/s)},\ z_r=5\ \text{(m)},\ \psi_d=1\ \text{(degree)}$$

In Figs. 14 (a)–(f), the red line is the proposed novel piecewise polynomial fuzzy time-delay network controller, and the blue line is the existing piecewise polynomial fuzzy time-delay network controller. In the figure, the response and convergence speed of the novel piecewise polynomial fuzzy delay controller is better than that of the existing delay controller, and it also converges faster than the existing controller when external disturbances. According to Fig. 15, the integrated square error of the coordinate and attitude of the proposed methods are smaller than those of the existing ones.

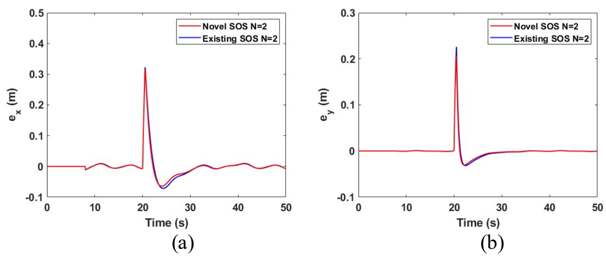

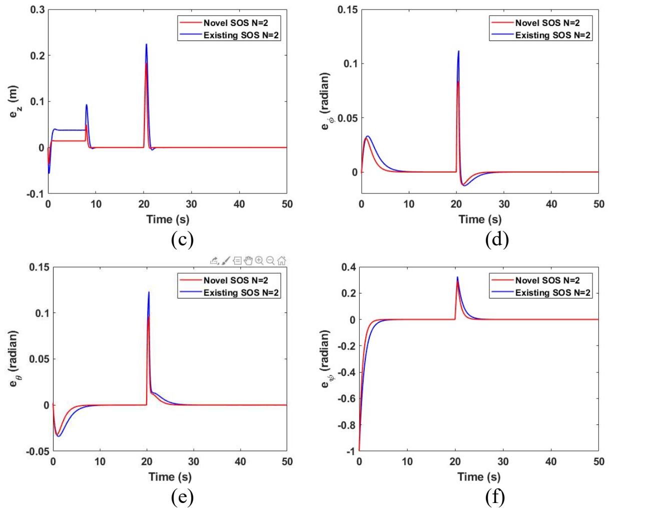

Fig. 14 (a) Time responses of $e_x(t)$. (b) Time responses of $e_y(t)$. (c) Time responses of $e_z(t)$. (d) Time responses of $e_\theta(t)$. (e) Time responses of $e_\phi(t)$. (f) Time responses of $e_\psi(t)$.

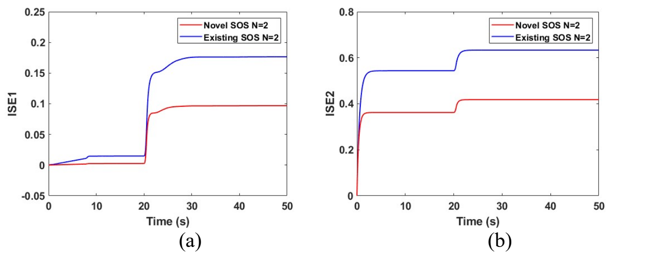

Fig. 15 (a) Time responses of coordinate of ISE. (b) Time responses of attitude of ISE.

Fig. 16 shows the tracking trajectory of the quadrotor. The black line represents the reference trajectory, the red line represents the trajectory of the proposed methods, and the blue line represents the trajectory of the existing methods. When the red line encounters a disturbance at 20 s, the speed of the red line returning to the reference trajectory is faster than that of the blue line.

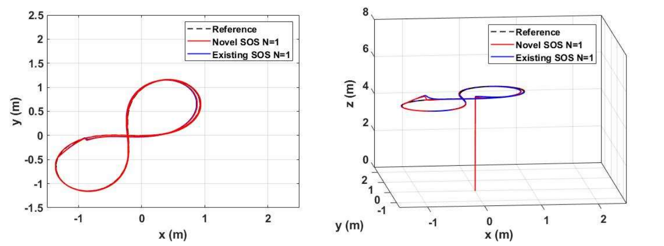

Fig. 16 (a) The trajectory of quadrotor in the x-y plane. (b) The trajectory of quadrotor in the 3D space.

Next, with the initial value $x=0$ (m), $y=0$ (m), $z=0$ (m), $\phi=0(\text{deg})$, $\theta=0(\text{deg})$, and $\psi=0(\text{deg})$ as the coordinate of the leader, $x=0$ (m), $y=-2$ (m), $z=0$ (m), $\phi=0(\text{deg})$, $\theta=0(\text{deg})$, and $\psi=0(\text{deg})$ as the coordinate and the desired formation of follower 1, $x=0$ (m), $y=2$ (m), $z=0$ (m), $\phi=0(\text{deg})$, $\theta=0(\text{deg})$, and $\psi=0(\text{deg})$ as the coordinate and the desired formation of follower 2, and 0.5 as the package dropout rate. In Figs. 17 (a)–(f), the error of the leader is shown in red, while the error of follower 1 is shown in blue, and the error of follower 2 is shown in green. The green line shows the smallest magnitude of oscillation because follower 2 was set as the smallest desired form. Fig. 18 shows the integrated square error of the coordinate and attitude.

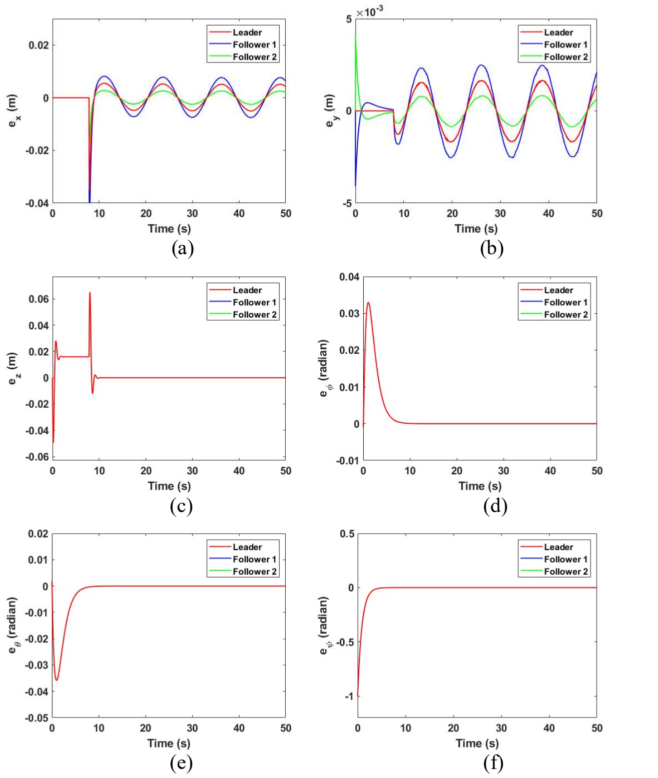

Fig. 17 (a) Time responses of $e_x(t)$. (b) Time responses of $e_y(t)$. (c) Time responses of $e_z(t)$. (d) Time responses of $e_\theta(t)$. (e) Time responses of $e_\phi(t)$. (f) Time responses of $e_\psi(t)$.

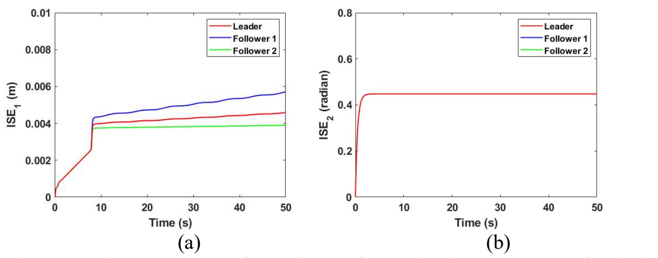

Fig. 18 (a) Time responses of coordinate of ISE. (b) Time responses of attitude of ISE.

Fig. 19 shows the tracking trajectory of quadrotors. The red line represents the tracking trajectory of the leader, the blue line represents the tracking trajectory of follower 1, and the green line represents the tracking trajectory of follower 2. According to the figure, the followers can effectively form a line formation with the leader.

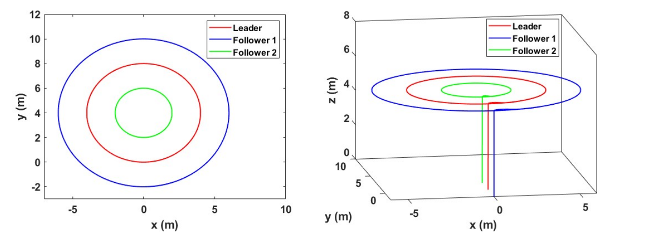

Fig. 19 (a) The trajectory of quadrotor in the x-y plane. (b) The trajectory of quadrotor in the 3D space.

Experiment Results

The proposed theorems are used to control the mobile robot and the quadrotor. Fig. 20 shows the C01 intelligent service robot. Fig. 21 (a) shows the ZD550 quadrotor, and the Mission Planner shows the trajectory of the quadrotor in Fig. 21 (b).

Fig. 20 The C01 mobile robot.

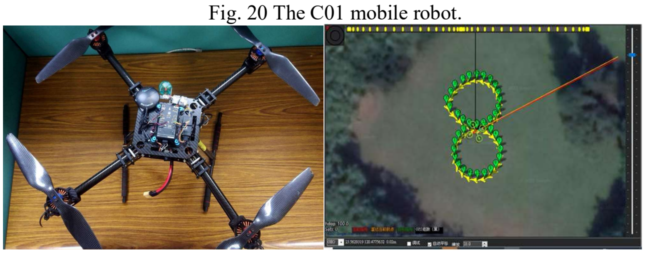

(a) (b)

Fig. 21 (a) The ZD550 quadrotor. (b) The trajectory in Mission Planner

(a) Mobile Robot

Assuming the initial condition of the robot is $x(0) = [0 \quad 0]^T$, and the consultation linear velocity and angular velocity are $v_r = 0.5(\text{m/s})$, and $\omega_r = -\sin(\frac{2\pi t}{15.118})(\text{rad/s})$. The external disturbance, which is defined as a pulse with an amplitude of 0.8 (m/s) and 0.8 (rad/sec) and occurred from the 10 s to the 11 s. The experimental results can be shown in Fig. 22 and Fig. 23.

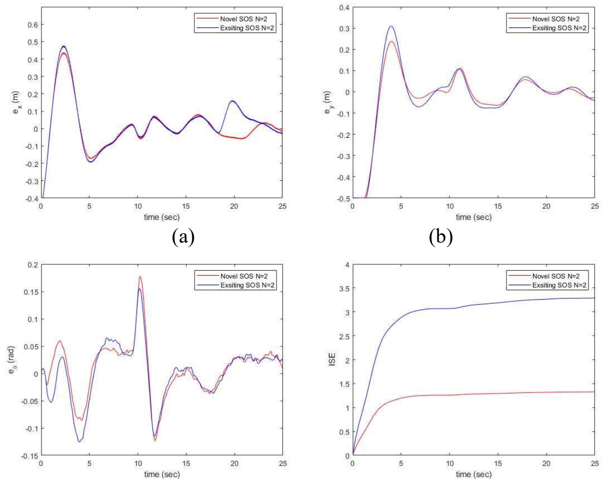

Fig .22 (a) Time responses of $e_x(t)$. (b) Time responses of $e_y(t)$. (c) Time responses of $e_\theta(t)$. (d) Time responses of ISE.

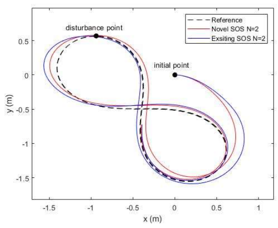

Fig .23 The trajectory of mobile robot.

From Fig. 22 and Fig. 23, better performance can be obtained by using the proposed method than by using the existing one in terms of tracking error and time response. The proposed method can resist external disturbance and also tolerate the model uncertainties.

(b) Quadrotor

Assuming the initial conditions of the quadrotor are $x = 0$ (m), $y = 0$ (m), $z = 0$ (m), $\phi = 0$ (rad), $\theta = 0$ (rad), $\psi = 0$ (rad). The consultation linear velocity and angular velocity are $v_r = 0.5$ (m/s) and $\omega_r = -\sin(\frac{2\pi t}{15.118})(\text{rad/s})$. The experimental results can be shown in Fig 24 to Fig. 26.

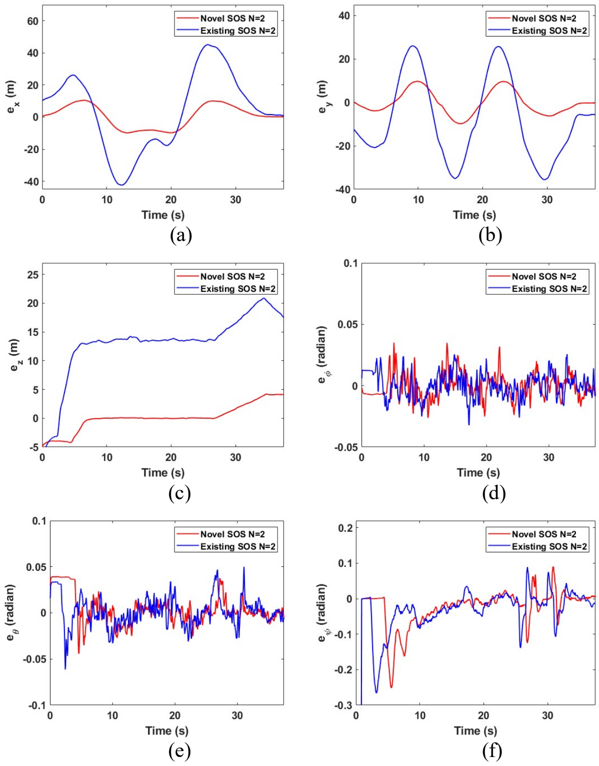

Fig. 24 (a) Time responses of $e_x(t)$. (b) Time responses of $e_y(t)$. (c) Time responses of $e_z(t)$. (d) Time responses of $e_\theta(t)$. (e) Time responses of $e_\phi(t)$. (f) Time responses of $e_\psi(t)$.

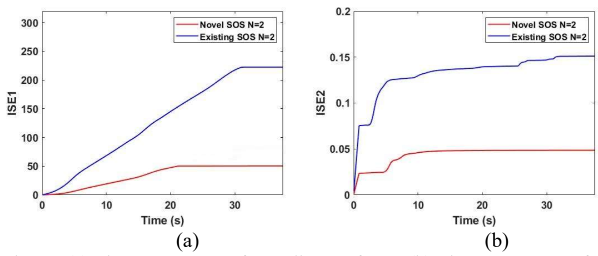

Fig. 25 (a) Time responses of coordinate of ISE. (b) Time responses of attitude of ISE.

Fig. 26 shows the tracking trajectory of the quadrotor. The black line represents the reference trajectory, the red line represents the trajectory of the proposed methods, and the blue line represents the trajectory of the existing methods. When the red line encounters a disturbance at 10 s, the speed of the red line returns to the reference trajectory faster than that of the blue line.

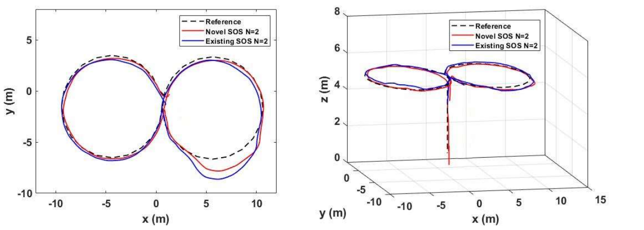

Fig. 26 (a) The trajectory of quadrotor in the x-y plane. (b) The trajectory of quadrotor in the 3D space.

From Fig. 24 to Fig. 26, a better performance can be obtained by using the proposed method than by using the existing one in terms of tracking error and time response. The proposed method can not only resist the external disturbance but also tolerate the model uncertainties.

VI. CONCLUSIONS

This study used the Minimum-Type PPLF to design the piecewise polynomial Lyapunov-Krasovskii functional function. Based on the plant delay as the basic environment, the output feedback was used to design a PPLF-based networked controller of polynomial fuzzy time-delay systems so that the system can avoid the disadvantages caused by using estimators. This system can reduce the number of rules, reduce the computational burden of the chip and make the system performance more excellent, and considers the network-induced package dropout and time delay, external disturbance, and model uncertainty. On the basis of a novel fuzzy model, the expanded feasible solution space allows the controller a greater chance of finding the best solution than a T–S fuzzy system. Finally, the designed controller was applied to trajectory tracking. The computer simulation and experimental results show that the PPLF-based networked controller of polynomial fuzzy time-delay systems is superior to the existing polynomial fuzzy time-delay network controller. Additionally, to describe the uncertainty of the communication channel of the network, the time delay and the package dropout during the networked control were considered in the proposed polynomial fuzzy formation networked control system. The design procedure was simplified by constructing a shifted team tracking dynamic system to track a fixed virtual structure formation. In the simulation result, the multi-agent networked system successfully achieves the expected form formation tracking with stable tracking performance.

REFERENCES

[1] R. Cioffi, M. Travaglioni, G. Piscitelli, A. Petrillo, and F. De Felice, “Artificial Intelligence and Machine Learning Applications in Smart Production: Progress, Trends, and Directions,” *Sustainability*, vol. 12, no. 2, p. 492, Jan. 2020.

[2] Y. He, C. Zhang, B. Wu, Y. Yang, K. Xiao and H. Li, "Cross-chain Trusted Service Quality Computing Scheme For Multi-chain Model-based 5G Network Slicing SLA," in *IEEE Internet of Things Journal*, 2021.

[3] X.-M. Zhang *et al.*, “Networked control systems: A survey of trends and techniques,” in *IEEE/CAA Journal of Automatica Sinica*, vol. 7, no. 1, pp. 1-17, 2019.

[4] J. Cervantes, W. Yu, S. Salazar and I. Chairez, “Takagi–Sugeno Dynamic Neuro-Fuzzy Controller of Uncertain Nonlinear Systems, ” in *IEEE Transactions on Fuzzy Systems*, vol. 25, no. 6, pp. 1601-1615, Dec. 2017,

[5] S. C. Mahto, R. M. Elavarasan, S. Ghosh, R. Saket, E. Hossain, and S. K. J. I. A. Nagar, “Improved stability criteria for time-varying delay system using second and first order polynomials,” in *IEEE Access*, vol. 8, pp. 210961-210969, 2020.

[6] Y. Liu, H. Gao, C. Zhai and W. Xie, “Internal Stability and String Stability of Connected Vehicle Systems With Time Delays, ” in *IEEE Transactions on Intelligent Transportation Systems*, vol. 22, no. 10, pp. 6162-6174, Oct. 2021.

[7] L. Zhu and C. J. A. Zhu, “An improved stability criterion for discrete-time time-delayed Lur'e system with sector-bounded nonlinearities,” *Automatika,* vol. 63, no. 2, pp. 216-225, 2022.

[8] J. Cervantes, W. Yu, S. Salazar, and I. J. I. T. o. F. S. Chairez, “Takagi–Sugeno dynamic neuro-fuzzy controller of uncertain nonlinear systems,” in *IEEE Transactions on Fuzzy Systems*, vol. 25, no. 6, pp. 1601-1615, 2016.

[9] R. Sakthivel, P. Selvaraj, B. J. I. T. o. S. Kaviarasan, Man,, and C. Systems, “Modified repetitive control design for nonlinear systems with time delay based on T–S fuzzy model,” in *IEEE Transactions on Systems, Man, and Cybernetics: Systems*, vol. 50, no. 2, pp. 646-655, 2017.

[10] S. Hwang and H. S. J. I. A. Kim, “Extended disturbance observer-based integral sliding mode control for nonlinear system via T–S fuzzy model,” in *IEEE Access*, vol. 8, pp. 116090-116105, 2020.

[11] T. Zhao, M. Huang, and S. J. I. T. o. F. S. Dian, “Robust stability and stabilization conditions for nonlinear networked control systems with network-induced delay via T–S fuzzy model,” in *IEEE Transactions on Fuzzy Systems*, vol. 29, no. 3, pp. 486-499, 2019.

[12] K. Tanaka, M. Tanaka, Y.-J. Chen, and H. O. J. I. T. o. F. S. Wang, “A new sum-of-squares design framework for robust control of polynomial fuzzy systems with uncertainties,” in *IEEE Transactions on Fuzzy Systems*, vol. 24, no. 1, pp. 94-110, 2015.

[13] F. Meng, D. Wang, P. Yang, G. Xie, and F. J. I. A. Guo, “Application of Sum-of-Squares Method in Estimation of Region of Attraction for Nonlinear Polynomial Systems,” in *IEEE Access*, vol. 8, pp. 14234-14243, 2020.

[14] Y. Zhao, Y. He, Z. Feng, P. Shi, and X. J. I. T. o. F. S. Du, “Relaxed sum-of-squares based stabilization conditions for polynomial fuzzy-model-based control systems,” in *IEEE Transactions on Fuzzy Systems*, vol. 27, no. 9, pp. 1767-1778, 2018.

[15] W.-B. Xie, S. Sang, H.-K. Lam, and J. J. I. T. o. F. S. Zhang, “A Polynomial Membership Function Approach for Stability Analysis of Fuzzy Systems,” in *IEEE Transactions on Fuzzy Systems*, vol. 29, no. 8, pp. 2077-2087, 2020.

[16] L. Teng, Y. Wang, W. Cai, and H. J. I. T. o. F. S. Li, “Robust fuzzy model predictive control of discrete-time Takagi–Sugeno systems with nonlinear local models,” in *IEEE Transactions on Fuzzy Systems*, vol. 26, no. 5, pp. 2915-2925, 2018.

[17] Y.-J. Chen, M. Tanaka, K. Tanaka, and H. O. Wang, “Piecewise polynomial lyapunov functions based stability analysis for polynomial fuzzy systems,” in *2013 IEEE International Conference on Control System, Computing and Engineering*, 2013, pp. 34-39.

[18] S. Ryszard, G. L. Demidova, D. V. J. J. S. Lukichev, M. Technical Of Information Technologies, and Optics, “Survey on fuzzy logic methods in control systems of electromechanical plants,” *Scientific and Technical Journal of Information Technologies, Mechanics and Optics*, vol. 119, no. 1, pp. 1-14, 2019.

[19] K. Tanaka, H. Yoshida, H. Ohtake and H. O. Wang, "A Sum-of-Squares Approach to Modeling and Control of Nonlinear Dynamical Systems With Polynomial Fuzzy Systems," in *IEEE Transactions on Fuzzy Systems*, vol. 17, no. 4, pp. 911-922, Aug. 2009.

[20] H.-N. Wu and H.-X. J. I. T. o. F. S. Li, “New approach to delay-dependent stability analysis and stabilization for continuous-time fuzzy systems with time-varying delay,” in *IEEE Transactions on Fuzzy Systems*, vol. 15, no. 3, pp. 482-493, 2007.

[21] J. Zhang and T. Raissi, "Indefinite Lyapunov–Razumikhin Functions-Based Stability and Event-Triggered Control of Switched Nonlinear Time-Delay Systems," in *IEEE Transactions on Circuits and Systems II: Express Briefs*, vol. 68, no. 10, pp. 3286-3290, Oct. 2021.

[22] H. Gassara, A. El Hajjaji, and M. J. I. J. o. S. S. Chaabane, “Design of polynomial fuzzy observer–controller for nonlinear systems with state delay: sum of squares approach,” *International Journal of Systems Science* 50:16, pages 2979-2992 vol. 48, no. 9, pp. 1954-1965, 2017.

[23] F. Aslam, F. Shoaib, H. Z. I. Khan, M. F. Haydar, and J. Riaz, “Robust Stability Analysis of an Uncertain Aircraft Model with Scalar Parametric Uncertainty,” in 2020 17th International Bhurban Conference on Applied Sciences and Technology (IBCAST), 2020: IEEE, pp. 296-302.

[24] X. Wang, Y. Zhou, Z. Zhao, W. Wei, and W. J. I. A. Li, “Time-delay system control based on an integration of active disturbance rejection and modified twice optimal control,” in *IEEE Access*, vol. 7, pp. 130734-130744, 2019.

[25] F. Wang, R. Wang, E. Liu, and W. J. I. A. Zhang, “Stabilization control mothed for two-axis inertially stabilized platform based on active

disturbance rejection control with noise reduction disturbance observer," in *IEEE Access*, vol. 7, pp. 99521-99529, 2019.

[26] S. Park and T. S. J. I. A. Yoon, "State space disturbance observer considering residual disturbance," in *IEEE Access*, vol. 8, pp. 213882-213886, 2020.

[27] Y. Zhao, Y. He, Z. Feng, P. Shi, and X. Du, "Relaxed sum-of-squares based stabilization conditions for polynomial fuzzy-model-based control systems," IEEE Trans. Fuzzy Syst., vol. 27, no. 9, pp. 1767-1778, 2018.

[28] Z. Chen, Q. Li, X. Ju, and F. J. I. A. Cen, "Barrier Lyapunov function-based sliding mode control for BWB aircraft with mismatched disturbances and output constraints," in *IEEE Access* vol. 7, pp. 175341-175352, 2019.

[29] X. Zong, T. Li, G. Yin and J. -F. Zhang, "Delay Tolerance for Stable Stochastic Systems and Extensions," in *IEEE Transactions on Automatic Control*, vol. 66, no. 6, pp. 2604-2619, June 2021.

[30] H. S. Kim, J. B. Park and Y. H. Joo, "A Fuzzy Lyapunov–Krasovskii Functional Approach to Sampled-Data Output-Feedback Stabilization of Polynomial Fuzzy Systems," in *IEEE Transactions on Fuzzy Systems*, vol. 26, no. 1, pp. 366-373, Feb. 2018.

[31] J. Umlauft, L. Pöhler, and S. J. I. C. S. L. Hirche, "An uncertainty-based control Lyapunov approach for control-affine systems modeled by Gaussian process," in *IEEE Control Systems Letters*, vol. 2, no. 3, pp. 483-488, 2018.

[32] Y. -Y. Wu and H. -J. Sun, "Attitude Tracking Control With Constraints for Rigid Spacecraft Based on Control Barrier Lyapunov Functions, " in *IEEE Transactions on Aerospace and Electronic Systems*, vol. 58, no. 3, pp. 2053- 2062, June 2022.

[33] B. Xiao, H.-K. Lam, Z. Zhong, and S. J. I. T. o. F. S. Wen, "Membership-function-dependent stabilization of event-triggered interval type-2 polynomial fuzzy-model-based networked control systems," in *IEEE Transactions on Fuzzy Systems*, vol. 28, no. 12, pp. 3171-3180, 2019.

[34] L. Rodrigues, J. Camino, and P. J. I.-P. Peres, "Gain-Scheduled H∞ Control for Discrete-Time Polynomial LPV Systems Using Homogeneous Polynomial Path-Dependent Lyapunov Functions," *IFAC-PapersOnLine,* vol. 51, no. 26, pp. 179-184, 2018.

[35] W. Li, Z. Xie, J. Zhao, P. K. Wong, H. Wang and X. Wang, "Static-Output-Feedback Based Robust Fuzzy Wheelbase Preview Control for Uncertain Active Suspensions With Time Delay and Finite Frequency Constraint," in *IEEE/CAA Journal of Automatica Sinica*, vol. 8, no. 3, pp. 664-678, March 2021.

[36] L. Li, G. Zhang and M. Ou, "A New Method to Non-Fragile Piecewise H∞ Control for Networked Nonlinear Systems With Packet Dropouts," in *IEEE Access*, vol. 8, pp. 196102-196111, 2020.

[37] L. Wang and H.-K. J. A. Lam, "H∞ control for continuous-time Takagi–Sugeno fuzzy model by applying generalized Lyapunov function and introducing outer variables," *Automatica,* vol. 125, p. 109409, 2021.

[38] M. -Y. Lee, B. -S. Chen, C. -Y. Tsai and C. -L. Hwang, "Stochastic H∞ Robust Decentralized Tracking Control of Large-Scale Team Formation UAV Network System With Time-Varying Delay and Package Dropout Under Interconnected Couplings and Wiener Fluctuations, " in *IEEE Access*, vol. 9, pp. 41976-41997, 2021.

[39] Z. Zhang, Z. Zhang, H. J. I. T. o. A. Zhang, and E. Systems, "Distributed attitude control for multispacecraft via Takagi–Sugeno fuzzy approach, " in *IEEE Transactions on Aerospace and Electronic Systems*, vol. 54, no. 2, pp. 642-654, 2017.

[40] Z. Zhang, Y. Shi, Z. Zhang, and W. J. I. T. o. C. Yan, "New results on sliding-mode control for Takagi–Sugeno fuzzy multiagent systems, " in *IEEE Transactions on Cybernetics*, vol. 49, no. 5, pp. 1592-1604, 2018.

[41] B.-S. Chen, C.-P. Wang, and M.-Y. J. I. T. o. C. Lee, "Stochastic robust team tracking control of multi-UAV networked system under Wiener and Poisson random fluctuations, " in *IEEE Transactions on Cybernetics*, vol. 51, no. 12, pp. 5786-5799, 2020.

[42] M.-Y. Lee, B.-S. Chen, Y. Chang, and C.-L. J. I. A. Hwang, "Stochastic robust team formation tracking design of multi-VTOL-UAV networked control system in smart city under time-varying delay and random fluctuation, " in *IEEE Access*, vol. 8, pp. 131310-131326, 2020.

[43] C.-j. Ru, R.-x. Wei, Y.-y. Wang, and J. J. M. P. i. E. Che, "Multimodel predictive control approach for UAV formation flight, " *Mathematical Problems in Engineering,* vol. 2014, 2014.

[44] H. Zhi, L. Chen, C. Li, Y. J. I. T. o. C. Guo, and S. I. E. Briefs, "Leader–Follower Affine Formation Control of Second-Order Nonlinear Uncertain Multi-Agent Systems, " in *IEEE Transactions on Circuits and Systems II: Express Briefs*, vol. 68, no. 12, pp. 3547-3551, 2021.

[45] F. Chen and D. V. J. I. T. o. C. o. N. S. Dimarogonas, "Leader–follower formation control with prescribed performance guarantees, " in *IEEE Transactions on Control of Network Systems*, vol. 8, no. 1, pp. 450-461, 2020.

APPENDIX

Lemma 1: Let Q be any of a $n \times n$ matrix. We have any constant $\beta > 0$ and any matrix $T > 0$ that

$$x^T Qz + z^T Q^T x \le \beta x^T Q T^{-1} Q^T x + \frac{1}{\beta} z^T T z \tag{58}$$

holds for all $x, z \in \Re^n$.

Lemma 2: For any constant symmetric matrix $N \in \Re^{n\times n}$, $N > 0$, scalar $\beta > 0$, vector function $\xi : [0, \beta] \to \Re^n$, such that the integrations are well defined as follows:

$$\beta \int_0^\beta \xi^T(\alpha) N \xi(\alpha) d\alpha \ge \left(\int_0^\beta \xi(\alpha) d\alpha \right)^T N \left(\int_0^\beta \xi(\alpha) d\alpha \right) \tag{59}$$

Lemma 3: For given the positive definite matrix Q, it will hold the following inequality for $t \in [t_k + \tau_k, t_{k+q} + \tau_{k+q})$.

$$\int_0^t \dot{x}(\sigma) Q \dot{x}(\sigma) d\sigma < \int_{t-\lambda}^t \dot{x}^T(\sigma) Q \dot{x}(\sigma) d\sigma \tag{60}$$

Lemma 4: For any real matrices X_{ij} for $i, j = 1, 2, ..., r$, and $\Lambda > 0$ with appropriate dimensions, it can be obtained as

$$\sum_{i=1}^r \sum_{j=1}^r \sum_{k=1}^r \sum_{l=1}^r h_i h_j h_k h_l X_{ij}^T \Lambda X_{kl} \le \sum_{i=1}^r \sum_{j=1}^r h_i h_j X_{ij}^T \Lambda X_{kl} \tag{61}$$

Lemma 5: Given real matrices $S = S^T$, M and N with appropriate dimensions, the following statement can be obtained:

There exists

$$S + MK(t)N + N^T K(t)^T M^T < 0 \tag{62}$$

for all $K(t)$ satisfying $K^T(t)K(t) \le I$, if and only if there exists any scalar $\kappa > 0$, such that

$$S + \kappa^{-1} M^T M + \kappa N^T N < 0 \tag{63}$$

Using Schur complement, (3-87) can be derived as

$$\begin{bmatrix} S & M & \kappa N^T \\ * & -\kappa I & 0 \\ * & * & -\kappa I \end{bmatrix} < 0 \tag{64}$$

(a) Proof1:

This is the derivation of the stability theorem of Theorem 1.

Take Lyapunov-Krasovskii piecewise polynomials functional as

$$\boldsymbol{V}_g(z) = z^{\mathrm{T}} \boldsymbol{P}_{\mathrm{g}}(\tilde{x}) z + \int_{-\lambda}^0 \int_{t+\omega}^t \dot{z}^{\mathrm{T}}(\sigma) \boldsymbol{Q}_{\mathrm{g}}(x) \dot{z}(\sigma) \mathrm{d}\sigma \mathrm{d}\omega + \int_{\mathrm{t}-\tau_e}^{\mathrm{t}} z^{\mathrm{T}}(\sigma) \boldsymbol{R}_{\mathrm{g}}(x) \dot{z}(\sigma) \mathrm{d}\sigma \tag{65}$$

Using the Newton-Leibniz formula $\boldsymbol{z}_k = \boldsymbol{z} - \int_{t_k}^t \dot{\boldsymbol{z}}(\boldsymbol{\sigma}) d\sigma$,, it is evident that, for any polynomial matrix $\boldsymbol{H}_{jg}(\boldsymbol{x})(j = 1, 2, 3)$ with the appropriate dimensions, we get

$$\left[z - z_{\mathrm{k}} - \int_{\mathrm{t_k}}^{\mathrm{t}} \dot{z}(\boldsymbol{\sigma}) \mathrm{d}\sigma \right]^{\mathrm{T}} \times \left[\boldsymbol{H}_{1\mathrm{g}}^{\mathrm{T}}(\boldsymbol{x}) z + \boldsymbol{H}_{2\mathrm{g}}^{\mathrm{T}}(\boldsymbol{x}) z_k + \boldsymbol{H}_{3\mathrm{g}}^{\mathrm{T}}(\boldsymbol{x}) \dot{z} \right] = 0 \tag{66}$$

$$\left[\boldsymbol{H}_{1g}^{\mathrm{T}}(\boldsymbol{x})z+\boldsymbol{H}_{2g}^{\mathrm{T}}(\boldsymbol{x})z_{k}+\boldsymbol{H}_{3g}^{\mathrm{T}}(\boldsymbol{x})\dot{z}\right]^{\mathrm{T}}\times\left[z-z_{k}-\int_{t_k}^{t}\dot{z}(\sigma)\mathrm{d}\sigma\right]=0 \tag{67}$$

Furthermore, based on (16), we can derive nonsingular matrix $\boldsymbol{G}_g(\tilde{\boldsymbol{x}})$ as follows:

$$\begin{aligned}&\left[\boldsymbol{G}_{g}^{\mathrm{T}}(\tilde{\boldsymbol{x}})z+\boldsymbol{G}_{g}^{\mathrm{T}}(\tilde{\boldsymbol{x}})z_{k}+\boldsymbol{G}_{g}^{\mathrm{T}}(\tilde{\boldsymbol{x}})\dot{z}\right]^{T}\\&\times\left\{\dot{z}-\sum_{i=1}^{2}\sum_{j=1}^{2}s_{i}s_{j}^{k}\left\{\begin{matrix}\left[\tilde{\boldsymbol{A}}_{i}(\boldsymbol{x})+\Delta\tilde{\boldsymbol{A}}_{i}\right]z+\left[\tilde{\boldsymbol{B}}_{i}(\boldsymbol{x})+\Delta\tilde{\boldsymbol{B}}_{i}\right]\boldsymbol{F}_{jg}(\boldsymbol{x})\boldsymbol{C}_{j}\boldsymbol{L}z_{k}\\+\tilde{\boldsymbol{D}}_{i}(\boldsymbol{x}(t))\boldsymbol{v}(t)\end{matrix}\right\}\right\}=0\end{aligned} \tag{68}$$

$$\begin{aligned}&\left\{\dot{z}-\sum_{i=1}^{2}\sum_{j=1}^{2}s_{i}s_{j}^{k}\left\{\begin{matrix}\left[\tilde{\boldsymbol{A}}_{i}(\boldsymbol{x})+\Delta\tilde{\boldsymbol{A}}_{i}\right]z+\left[\tilde{\boldsymbol{B}}_{i}(\boldsymbol{x})+\Delta\tilde{\boldsymbol{B}}_{i}\right]\boldsymbol{F}_{jg}(\boldsymbol{x})\boldsymbol{C}_{j}\boldsymbol{L}z_{k}\\+\tilde{\boldsymbol{D}}_{i}(\boldsymbol{x}(t))\boldsymbol{v}(t)\end{matrix}\right\}\right\}^{T}\\&\times\left[\boldsymbol{G}_{g}^{\mathrm{T}}(\tilde{\boldsymbol{x}})z+\boldsymbol{G}_{g}^{\mathrm{T}}(\tilde{\boldsymbol{x}})z_{k}+\boldsymbol{G}_{g}^{\mathrm{T}}(\tilde{\boldsymbol{x}})\dot{z}\right]=0\end{aligned} \tag{69}$$

The time derivative of $\boldsymbol{P}_g(\tilde{\boldsymbol{x}})$ can be derived as follows:

$$\dot{\boldsymbol{P}}_{g}(\tilde{\boldsymbol{x}})=\sum_{l\in L}\frac{\partial\boldsymbol{P}_{g}}{\partial x_{l}}(\tilde{\boldsymbol{x}})\tilde{\boldsymbol{A}}_{i}^{l}(\boldsymbol{x})\hat{x} \tag{70}$$

Since $\tilde{\boldsymbol{B}}_i^l(\boldsymbol{x})=0$ for $l\in\boldsymbol{L}$, the following equation can be obtained:

$$\dot{\boldsymbol{x}}_{l}=\sum_{i=1}^{2}s_{i}\tilde{\boldsymbol{A}}_{i}^{l}(\boldsymbol{x})\hat{\boldsymbol{x}} \tag{72}$$

On the other hand

$$\frac{\partial\boldsymbol{P}_{g}}{\partial x_{l}}(\tilde{\boldsymbol{x}})=0 \tag{73}$$

Combining (65)–(70), the time derivative of $\boldsymbol{V}_g(z)$, for $t\in\left[t_k+\tau_k,t_{k+q}+\tau_{k+q}\right)$ is obtained as

$$\begin{aligned}\dot{\boldsymbol{V}}_{g}(z)\le\;&\dot{z}^{T}\boldsymbol{P}_{g}(\tilde{x})z+z^{T}\boldsymbol{P}_{g}(\tilde{x})\dot{z}+z^{T}\dot{\boldsymbol{P}}_{g}(\tilde{x})z+\lambda\dot{z}^{T}\boldsymbol{Q}_{g}(x)\dot{z}\\&+z^{T}\boldsymbol{R}_{g}(\tilde{x})z-z_{\tau}^{T}\boldsymbol{R}_{g}(\tilde{x})z_{\tau}-\int_{t-\lambda}^{t}\dot{z}^{T}(\sigma)\boldsymbol{Q}_{g}(x)\dot{z}(\sigma)d\sigma\\&+\left[z-z_{k}-\int_{t_k}^{t}\dot{z}(\sigma)d\sigma\right]^{T}\times\left[\boldsymbol{H}_{1g}^{T}(x)z+\boldsymbol{H}_{2g}^{T}(x)z_{k}+\boldsymbol{H}_{3g}^{T}(x)\dot{z}\right]\\&+\left[\boldsymbol{H}_{1g}^{T}(x)z+\boldsymbol{H}_{2g}^{T}(x)z_{k}+\boldsymbol{H}_{3g}^{T}(x)\dot{z}\right]^{T}\times\left[z-z_{k}-\int_{t_k}^{t}\dot{z}(\sigma)d\sigma\right]\\&+\left[\boldsymbol{G}_{g}^{T}(\tilde{x})z+\boldsymbol{G}_{g}^{T}(\tilde{x})z_{k}+\boldsymbol{G}_{g}^{T}(\tilde{x})\dot{z}\right]^{T}\\&\times\left\{\dot{z}-\sum_{i=1}^{2}\sum_{j=1}^{2}s_{i}s_{j}^{k}\left\{\begin{matrix}\left[\tilde{\boldsymbol{A}}_{i}(x)+\Delta\tilde{\boldsymbol{A}}_{i}\right]z+\left[\tilde{\boldsymbol{B}}_{i}(x)+\Delta\tilde{\boldsymbol{B}}_{i}\right]\boldsymbol{F}_{jg}(x)\boldsymbol{C}_{j}\boldsymbol{L}z_{k}\\+\tilde{\boldsymbol{D}}_{i}(\boldsymbol{x}(t))\boldsymbol{v}(t)\end{matrix}\right\}\right\}\\&+\left\{\dot{z}-\sum_{i=1}^{2}\sum_{j=1}^{2}s_{i}s_{j}^{k}\left\{\begin{matrix}\left[\tilde{\boldsymbol{A}}_{i}(x)+\Delta\tilde{\boldsymbol{A}}_{i}\right]z+\left[\tilde{\boldsymbol{B}}_{i}(x)+\Delta\tilde{\boldsymbol{B}}_{i}\right]\boldsymbol{F}_{jg}(x)\boldsymbol{C}_{j}\boldsymbol{L}z_{k}\\+\tilde{\boldsymbol{D}}_{i}(\boldsymbol{x}(t))\boldsymbol{v}(t)\end{matrix}\right\}\right\}^{T}\\&\times\left[\boldsymbol{G}_{g}^{T}(\tilde{x})z+\boldsymbol{G}_{g}^{T}(\tilde{x})z_{k}+\boldsymbol{G}_{g}^{T}(\tilde{x})\dot{z}\right]\\&+\sum_{g=1}^{N}\lambda_{g}\hat{\boldsymbol{x}}^{T}(x)\left(\boldsymbol{P}_{q}(\tilde{x})-\boldsymbol{P}_{g}(\tilde{x})\right)\hat{\boldsymbol{x}}(x)\end{aligned} \tag{74}$$

Utilizing *Lemma 1*, *Lemma 2* and *Lemma 3*, (66) and (67) can be derived as

$$\begin{aligned}&-\left[\boldsymbol{H}_{1g}^{T}(\boldsymbol{x})z+\boldsymbol{H}_{2g}^{T}(\boldsymbol{x})z_{k}+\boldsymbol{H}_{3g}^{T}(\boldsymbol{x})\dot{z}\right]^{T}\times\int_{t_k}^{t}\dot{z}(\sigma)d\sigma\\&-\int_{t_k}^{t}\dot{z}^{T}(\sigma)d\sigma\times\left[\boldsymbol{H}_{1g}^{T}(\boldsymbol{x})z+\boldsymbol{H}_{2g}^{T}(\boldsymbol{x})z_{k}+\boldsymbol{H}_{3g}^{T}(\boldsymbol{x})\dot{z}\right]\\&\le\lambda\eta^{T}\hat{\boldsymbol{H}}_{g}(\boldsymbol{x})\boldsymbol{Q}_{g}^{-1}(\boldsymbol{x})\hat{\boldsymbol{H}}_{g}^{T}(\boldsymbol{x})\eta+\frac{1}{\lambda}\left(\int_{t_k}^{t}\dot{z}(\sigma)\boldsymbol{d}\sigma\right)^{T}\boldsymbol{Q}_{g}(\boldsymbol{x})\left(\int_{t_k}^{t}\dot{z}(\sigma)\boldsymbol{d}\sigma\right)\\&\le\lambda\eta^{T}\hat{\boldsymbol{H}}_{g}(\boldsymbol{x})\boldsymbol{Q}_{g}^{-1}(\boldsymbol{x})\hat{\boldsymbol{H}}_{g}^{T}(\boldsymbol{x})\eta+\frac{t-t_{k}}{\lambda}\int_{t_k}^{t}\dot{z}^{T}(\sigma)\boldsymbol{Q}_{g}(\boldsymbol{x})\dot{z}(\sigma)\boldsymbol{d}\sigma\\&\le\lambda\eta^{T}\hat{\boldsymbol{H}}_{g}(\boldsymbol{x})\boldsymbol{Q}_{g}^{-1}(\boldsymbol{x})\hat{\boldsymbol{H}}_{g}^{T}(\boldsymbol{x})\eta+\int_{t-\lambda}^{t}\dot{z}^{T}(\sigma)\boldsymbol{Q}_{g}(\boldsymbol{x})\dot{z}(\sigma)\boldsymbol{d}\sigma\end{aligned} \tag{75}$$

where

$\hat{\boldsymbol{H}}_{g}^{\mathrm{T}}(x)=\left[\boldsymbol{H}_{1g}^{\mathrm{T}}\quad\boldsymbol{H}_{2g}^{\mathrm{T}}\quad\boldsymbol{H}_{3g}^{\mathrm{T}}\quad0\quad0\right]$, $\boldsymbol{\eta}^{\mathrm{T}}=\left[z^{\mathrm{T}}\quad z_{k}^{\mathrm{T}}\quad\dot{z}^{\mathrm{T}}\quad z_{\tau}^{\mathrm{T}}\quad v^{\mathrm{T}}\right]$, $\exists\lambda>0,\ \exists\boldsymbol{Q}_{g}>0$.

Substituting the result of (75) into (74), the inequality can be rewritten as follows:

$$\begin{aligned}\dot{\boldsymbol{V}}_{g}(z)<\;&\dot{z}^{T}\boldsymbol{P}_{g}(\tilde{x})z+z^{T}\boldsymbol{P}_{g}(\tilde{x})\dot{z}+z^{T}\dot{\boldsymbol{P}}_{g}(\tilde{x})z+\lambda\dot{z}^{T}\boldsymbol{Q}_{g}(x)\dot{z}\\&+z^{T}\boldsymbol{R}_{g}(\tilde{x})z_{t}-z_{\tau}^{T}\boldsymbol{R}_{g}(\tilde{x})z_{\tau}+\lambda\eta^{T}\hat{\boldsymbol{H}}_{g}(x)\boldsymbol{Q}_{g}^{-1}(x)\hat{\boldsymbol{H}}_{g}^{T}(x)\eta\\&-\int_{t-\lambda}^{t}\dot{z}^{T}(\sigma)\boldsymbol{Q}_{g}(x)\dot{z}(\sigma)\boldsymbol{d}\sigma+\int_{t-\lambda}^{t}\dot{z}^{T}(\sigma)\boldsymbol{Q}_{g}(x)\dot{z}(\sigma)\boldsymbol{d}\sigma\\&+\left[z-z_{k}\right]^{T}\times\left[\boldsymbol{H}_{1g}^{T}(x)z+\boldsymbol{H}_{2g}^{T}(x)z_{k}+\boldsymbol{H}_{3g}^{T}(x)\dot{z}\right]\\&+\left[\boldsymbol{H}_{1g}^{T}(x)z+\boldsymbol{H}_{2g}^{T}(x)z_{k}+\boldsymbol{H}_{3g}^{T}(x)\dot{z}\right]^{T}\times\left[z-z_{k}\right]\\&+\left[\boldsymbol{G}_{g}^{T}(\tilde{x})z+\boldsymbol{G}_{g}^{T}(\tilde{x})z_{k}+\boldsymbol{G}_{g}^{T}(\tilde{x})\dot{z}\right]^{T}\\&\times\left\{\dot{z}-\sum_{i=1}^{2}\sum_{j=1}^{2}s_{i}s_{j}^{k}\left\{\begin{matrix}\left[\tilde{\boldsymbol{A}}_{i}(x)+\Delta\tilde{\boldsymbol{A}}_{i}\right]z+\left[\tilde{\boldsymbol{B}}_{i}(x)+\Delta\tilde{\boldsymbol{B}}_{i}\right]\boldsymbol{F}_{jg}(x)\boldsymbol{C}_{j}\boldsymbol{L}z_{k}\\+\tilde{\boldsymbol{D}}_{i}(\boldsymbol{x}(t))\boldsymbol{v}(t)\end{matrix}\right\}\right\}\\&+\left\{\dot{z}-\sum_{i=1}^{2}\sum_{j=1}^{2}s_{i}s_{j}^{k}\left\{\begin{matrix}\left[\tilde{\boldsymbol{A}}_{i}(x)+\Delta\tilde{\boldsymbol{A}}_{i}\right]z+\left[\tilde{\boldsymbol{B}}_{i}(x)+\Delta\tilde{\boldsymbol{B}}_{i}\right]\boldsymbol{F}_{jg}(x)\boldsymbol{C}_{j}\boldsymbol{L}z_{k}\\+\tilde{\boldsymbol{D}}_{i}(\boldsymbol{x}(t))\boldsymbol{v}(t)\end{matrix}\right\}\right\}^{T}\\&\times\left[\boldsymbol{G}_{g}^{T}(\tilde{x})z+\boldsymbol{G}_{g}^{T}(\tilde{x})z_{k}+\boldsymbol{G}_{g}^{T}(\tilde{x})\dot{z}\right]\\&+\sum_{g=1}^{N}\lambda_{g}\hat{\boldsymbol{x}}^{T}(x)\left(\boldsymbol{P}_{g}(\tilde{x})-\boldsymbol{P}_{q}(\tilde{x})\right)\hat{\boldsymbol{x}}(x)\end{aligned}$$

(76)

Moreover, the inequality can be reorganized by rewriting (76) with η as follows:

$$\begin{aligned}\dot{\boldsymbol{V}}_{g}(z)<\sum_{i=1}^{2}\sum_{j=1}^{2}s_{i}s_{j}^{k}\Big\{&\\&\boldsymbol{\eta}^{T}\begin{bmatrix}\sum_{l\in\boldsymbol{L}}\frac{\partial\boldsymbol{P}_{g}}{\partial\boldsymbol{x}_{l}}(\tilde{x})\tilde{\boldsymbol{A}}_{i}^{l}(\boldsymbol{x})\hat{x}+\sum_{g=1}^{N}\lambda_{g}\boldsymbol{L}^{T}\left[\boldsymbol{P}_{q}(\tilde{x})-\boldsymbol{P}_{g}(\tilde{x})\right]\boldsymbol{L}+\boldsymbol{R}_{g} & 0 & \boldsymbol{P}_{g}(\tilde{x}) & 0\\0 & 0 & 0 & 0\\\boldsymbol{P}_{g}(\tilde{x}) & 0 & \lambda\boldsymbol{Q}_{g}(\boldsymbol{x}) & 0\\0 & 0 & 0 & -\boldsymbol{R}_{g}(\boldsymbol{x})\end{bmatrix}\boldsymbol{\eta}\\&+\boldsymbol{\eta}^{T}\begin{bmatrix}\boldsymbol{H}_{1g}(\boldsymbol{x}) & -\boldsymbol{H}_{1g}(\boldsymbol{x}) & 0 & 0\\\boldsymbol{H}_{2g}(\boldsymbol{x}) & -\boldsymbol{H}_{2g}(\boldsymbol{x}) & 0 & 0\\\boldsymbol{H}_{3g}(\boldsymbol{x}) & -\boldsymbol{H}_{3g}(\boldsymbol{x}) & 0 & 0\\0 & 0 & 0 & 0\end{bmatrix}\eta+\eta^{T}\begin{bmatrix}\boldsymbol{H}_{1g}(\boldsymbol{x}) & -\boldsymbol{H}_{1g}(\boldsymbol{x}) & 0 & 0\\\boldsymbol{H}_{2g}(\boldsymbol{x}) & -\boldsymbol{H}_{2g}(\boldsymbol{x}) & 0 & 0\\\boldsymbol{H}_{3g}(\boldsymbol{x}) & -\boldsymbol{H}_{3g}(\boldsymbol{x}) & 0 & 0\\0 & 0 & 0 & 0\end{bmatrix}^{T}\boldsymbol{\eta}\\&+\boldsymbol{\eta}^{T}\begin{bmatrix}-\boldsymbol{G}_{g}(\tilde{x})[\tilde{\boldsymbol{A}}_{i}(\boldsymbol{x})+\Delta\tilde{\boldsymbol{A}}_{i}] & -\boldsymbol{G}_{g}(\tilde{x})[\tilde{\boldsymbol{B}}_{i}(\boldsymbol{x})+\Delta\tilde{\boldsymbol{B}}_{i}]\boldsymbol{F}_{jg}(\boldsymbol{x})\boldsymbol{C}_{j}\boldsymbol{L} & \boldsymbol{G}_{g}(\tilde{x}) & 0\\-\boldsymbol{G}_{g}(\tilde{x})[\tilde{\boldsymbol{A}}_{i}(\boldsymbol{x})+\Delta\tilde{\boldsymbol{A}}_{i}] & -\boldsymbol{G}_{g}(\tilde{x})[\tilde{\boldsymbol{B}}_{i}(\boldsymbol{x})+\Delta\tilde{\boldsymbol{B}}_{i}]\boldsymbol{F}_{jg}(\boldsymbol{x})\boldsymbol{C}_{j}\boldsymbol{L} & \boldsymbol{G}_{g}(\tilde{x}) & 0\\-\boldsymbol{G}_{g}(\tilde{x})[\tilde{\boldsymbol{A}}_{i}(\boldsymbol{x})+\Delta\tilde{\boldsymbol{A}}_{i}] & -\boldsymbol{G}_{g}(\tilde{x})[\tilde{\boldsymbol{B}}_{i}(\boldsymbol{x})+\Delta\tilde{\boldsymbol{B}}_{i}]\boldsymbol{F}_{jg}(\boldsymbol{x})\boldsymbol{C}_{j}\boldsymbol{L} & \boldsymbol{G}_{g}(\tilde{x}) & 0\\0 & 0 & 0 & 0\end{bmatrix}\boldsymbol{\eta}\\&+\boldsymbol{\eta}^{T}\begin{bmatrix}-\boldsymbol{G}_{g}(\tilde{x})[\tilde{\boldsymbol{A}}_{i}(\boldsymbol{x})+\Delta\tilde{\boldsymbol{A}}_{i}] & -\boldsymbol{G}_{g}(\tilde{x})[\tilde{\boldsymbol{B}}_{i}(\boldsymbol{x})+\Delta\tilde{\boldsymbol{B}}_{i}]\boldsymbol{F}_{jg}(\boldsymbol{x})\boldsymbol{C}_{j}\boldsymbol{L} & \boldsymbol{G}_{g}(\tilde{x}) & 0\\-\boldsymbol{G}_{g}(\tilde{x})[\tilde{\boldsymbol{A}}_{i}(\boldsymbol{x})+\Delta\tilde{\boldsymbol{A}}_{i}] & -\boldsymbol{G}_{g}(\tilde{x})[\tilde{\boldsymbol{B}}_{i}(\boldsymbol{x})+\Delta\tilde{\boldsymbol{B}}_{i}]\boldsymbol{F}_{jg}(\boldsymbol{x})\boldsymbol{C}_{j}\boldsymbol{L} & \boldsymbol{G}_{g}(\tilde{x}) & 0\\-\boldsymbol{G}_{g}(\tilde{x})[\tilde{\boldsymbol{A}}_{i}(\boldsymbol{x})+\Delta\tilde{\boldsymbol{A}}_{i}] & -\boldsymbol{G}_{g}(\tilde{x})[\tilde{\boldsymbol{B}}_{i}(\boldsymbol{x})+\Delta\tilde{\boldsymbol{B}}_{i}]\boldsymbol{F}_{jg}(\boldsymbol{x})\boldsymbol{C}_{j}\boldsymbol{L} & \boldsymbol{G}_{g}(\tilde{x}) & 0\\0 & 0 & 0 & 0\end{bmatrix}^{T}\boldsymbol{\eta}\\&+\boldsymbol{\eta}^{T}\begin{bmatrix}\boldsymbol{L}^{T}\boldsymbol{C}_{i}^{T}\boldsymbol{C}_{i}\boldsymbol{L} & 0 & 0 & 0 & 0\\0 & 0 & 0 & 0 & 0\\0 & 0 & 0 & 0 & 0\\0 & 0 & 0 & 0 & 0\\0 & 0 & 0 & 0 & -\gamma^{2}\boldsymbol{I}\end{bmatrix}^{T}\boldsymbol{\eta}\\&+\lambda\boldsymbol{\eta}^{T}\hat{\boldsymbol{H}}_{g}(\boldsymbol{x})\boldsymbol{Q}_{g}^{-1}(\boldsymbol{x})\hat{\boldsymbol{H}}_{g}^{T}(\boldsymbol{x})\boldsymbol{\eta}\Big\}\end{aligned} \tag{77}$$

Rewrite (77) into the form as follows:

$$\dot{V}_g(z) < \sum_{i=1}^{2}\sum_{j=1}^{2} s_i s_j^k \eta^T \left[\tilde{\Xi}_{ijg} + \lambda \hat{H}_g(x) Q_g^{-1}(x) \hat{H}_g^T(x)\right]\eta \quad (78)$$

where

$$\tilde{\Xi}_{\mathrm{ijg}} = \begin{bmatrix} \tilde{\Xi}_{11\mathrm{g}} + L^{\mathrm{T}} C_{\mathrm{i}}^{\mathrm{T}} C_{\mathrm{i}} L & \tilde{\Xi}_{12\mathrm{g}} & \tilde{\Xi}_{13\mathrm{g}} & 0 & -G_{\mathrm{g}}(\tilde{x}) \tilde{D}_{\mathrm{i}}(x(\mathrm{t})) \\ * & \tilde{\Xi}_{22\mathrm{g}} & \tilde{\Xi}_{23\mathrm{g}} & 0 & -G_{\mathrm{g}}(\tilde{x}) \tilde{D}_{\mathrm{i}}(x(\mathrm{t})) \\ * & * & \tilde{\Xi}_{33\mathrm{g}} & 0 & -G_{\mathrm{g}}(\tilde{x}) \tilde{D}_{\mathrm{i}}(x(\mathrm{t})) \\ * & * & * & \tilde{\Xi}_{44\mathrm{g}} & 0 \\ * & * & * & * & -\gamma^2 I \end{bmatrix}$$

$$\tilde{\Xi}_{11g} = \sum_{l \in L} \frac{\partial P_g}{\partial x_l}(\tilde{x}) \tilde{A}_i^l(x)\hat{x} + H_{1g}(x) + H_{1g}^T(x) - G_g(\tilde{x})\left[\tilde{A}_i(x) + \Delta\tilde{A}_i\right]$$
$$-\left[\tilde{A}_i(x) + \Delta\tilde{A}_i\right]^T(x) G_g^T(\tilde{x}) + \sum_{g=1}^{N} \lambda_g L^T\left[P_q(\tilde{x}) - P_g(\tilde{x})\right] L + R_g$$

$$\tilde{\Xi}_{12g} = H_{2g}^T(x) - H_{1g}(x) - G_g(\tilde{x})\left[\tilde{B}_i(x) + \Delta\tilde{B}_i\right] F_{jg}(x) C_j L - \left[\tilde{A}_i(x) + \Delta\tilde{A}_i\right]^T(x) G_g^T(\tilde{x})$$

$$\tilde{\Xi}_{13g} = P_g(\tilde{x}) + H_{3g}^T(x) + G_g(\tilde{x}) - \left[\tilde{A}_i(x) + \Delta\tilde{A}_i\right]^T(x) G_g^T(\tilde{x})$$

$$\tilde{\Xi}_{22g} = -H_{2g}(x) - H_{2g}^T(x) - G_g(\tilde{x})\left[\tilde{B}_i(x) + \Delta\tilde{B}_i\right] F_{jg}(x) C_j L$$
$$- L^T C_j^T F_{jg}^T(x)\left[\tilde{B}_i(x) + \Delta\tilde{B}_i\right]^T(x) G_g^T(\tilde{x})$$

$$\tilde{\Xi}_{23g} = G_g(\tilde{x}) - H_{3g}^T(x) - L^T C_j^T F_{jg}^T(x)\left[\tilde{B}_i(x) + \Delta\tilde{B}_i\right]^T(x) G_g^T(\tilde{x})$$

$$\tilde{\Xi}_{33g} = \lambda Q_g(x) + G_g(\tilde{x}) + G_g^T(\tilde{x})$$

$$\tilde{\Xi}_{44g} = -R_g(x)$$

Consider H_∞ performance index such as (15). The following inequality can be expressed as

$$\dot{V}_g(x) + y^T y - \gamma^2 v^T v < 0 \quad (79)$$

Based on (77) and (79), the inequality is obtained as follows

$$\sum_{i=1}^{2}\sum_{j=1}^{2} \mathrm{s_i s_j^k} \eta^{\mathrm{T}} \left[\tilde{\Xi}_{\mathrm{ijg}} + \lambda \hat{H}_{\mathrm{g}}(x) Q_{\mathrm{g}}^{-1}(x) \hat{H}_{\mathrm{g}}^{\mathrm{T}}(x)\right]\eta < 0 \quad (80)$$

If $\tilde{\Xi}_{ijg}(x) + \lambda \hat{H}_g(x) Q_g^{-1}(x) \hat{H}_g^T(x) < 0$ is satisfied for $i \le j$, it means $\dot{V}_g(z) < 0$.

The inequality can be obtained as (81) by using the Schur complement.

$$\dot{V}_g(z) < \sum_{i=1}^{2}\sum_{j=1}^{2} s_i s_j^k \eta^T \tilde{\Phi}_{ijg}(x)\eta \quad (81)$$

where

$$\tilde{\Phi}_{ijg}(x) = \begin{bmatrix} \tilde{\Xi}_{11g} & \tilde{\Xi}_{12g} & \tilde{\Xi}_{13g} & 0 & -G_g(\tilde{x})\tilde{D}_i(x(t)) & \lambda H_{1g}(x) & L^T C_i^T(x) \\ * & \tilde{\Xi}_{22g} & \tilde{\Xi}_{23g} & 0 & -G_g(\tilde{x})\tilde{D}_i(x(t)) & \lambda H_{2g}(x) & 0 \\ * & * & \tilde{\Xi}_{33g} & 0 & -G_g(\tilde{x})\tilde{D}_i(x(t)) & \lambda H_{3g}(x) & 0 \\ * & * & * & \tilde{\Xi}_{44g} & 0 & 0 & 0 \\ * & * & * & * & -\gamma^2 I & 0 & 0 \\ * & * & * & * & * & -\lambda Q_g(x) & 0 \\ * & * & * & * & * & * & -I \end{bmatrix} \quad (82)$$

The transposed matrix at the symmetrical position is denoted as *.

For brevity, $\tilde{\Phi}_{ijg}(x)$ will be separated into two parts. $\hat{\Phi}_{ijg}(x)$ is the term without model uncertainties. $\Delta\tilde{\Phi}_{ijg}(x)$ is the model uncertainties term. Thus

$$\tilde{\Phi}_{\mathrm{ijg}}(x) = \hat{\Phi}_{\mathrm{ijg}}(x) + \Delta\tilde{\Phi}_{\mathrm{ijg}}(x) \quad (83)$$

among them

$$\hat{\Phi}_{ijg}(x) = \begin{bmatrix} \hat{\Xi}_{11g} & \hat{\Xi}_{12g} & \hat{\Xi}_{13g} & 0 & -G_g(\tilde{x})\tilde{D}_i(x(t)) & \lambda H_{1g}(x) & L^T C_i^T(x) \\ * & \hat{\Xi}_{22g} & \hat{\Xi}_{23g} & 0 & -G_g(\tilde{x})\tilde{D}_i(x(t)) & \lambda H_{2g}(x) & 0 \\ * & * & \hat{\Xi}_{33g} & 0 & -G_g(\tilde{x})\tilde{D}_i(x(t)) & \lambda H_{3g}(x) & 0 \\ * & * & * & \hat{\Xi}_{44g} & 0 & 0 & 0 \\ * & * & * & * & -\gamma^2 I & 0 & 0 \\ * & * & * & * & * & -\lambda Q_g(x) & 0 \\ * & * & * & * & * & * & -I \end{bmatrix} \quad (84)$$

The transposed matrix at the symmetrical position is denoted as *.

$$\hat{\Xi}_{11g} = \sum_{l \in L} \frac{\partial P_g}{\partial x_l}(\tilde{x}) \tilde{A}_i^l(x)\hat{x} + H_{1g}(x) + H_{1g}^T(x) - G_g(\tilde{x}) \tilde{A}_i(x)$$
$$- \tilde{A}_i(x) G_g^T(\tilde{x}) + \sum_{g=1}^{N} \lambda_g L^T\left[P_q(\tilde{x}) - P_g(\tilde{x})\right] L + R_g(x)$$

$$\hat{\Xi}_{12g} = H_{2g}^T(x) - H_{1g}(x) - G_g(\tilde{x}) \tilde{B}_i^T(x) F_{jg}(x) C_j L - \tilde{A}_i(x) G_g^T(\tilde{x})$$

$$\hat{\Xi}_{13g} = P_g(\tilde{x}) + H_{3g}^T(x) + G_g(\tilde{x}) - \tilde{A}_i(x) G_g^T(\tilde{x})$$

$$\hat{\Xi}_{22g} = -H_{2g}(x) - H_{2g}^T(x) - G_g(\tilde{x}) \tilde{B}_i^T(x) F_{jg}(x) C_j L - L^T C_j^T F_{jg}^T(x) \tilde{B}_i^T(x) G_g^T(\tilde{x})$$

$$\hat{\Xi}_{23g} = G_g(\tilde{x}) - H_{3g}^T(x) - L^T C_j^T F_{jg}^T(x) \tilde{B}_i^T(x) G_g^T(\tilde{x})$$

$$\hat{\Xi}_{33g} = \lambda Q_g(x) + G_g(\tilde{x}) + G_g^T(\tilde{x})$$

$$\hat{\Xi}_{44g} = -R_g(x)$$

$$\Delta\tilde{\Phi}_{ijg}(x) = \begin{bmatrix} -G_g(\tilde{x})\Delta\tilde{A}_i & -G_g(\tilde{x})\Delta\tilde{B}_i\tilde{F}_{jg}(x)C_j L & 0 & 0 & 0 & 0 & 0 \\ -G_g(\tilde{x})\Delta\tilde{A}_i & -G_g(\tilde{x})\Delta\tilde{B}_i\tilde{F}_{jg}(x)C_j L & 0 & 0 & 0 & 0 & 0 \\ -G_g(\tilde{x})\Delta\tilde{A}_i & -G_g(\tilde{x})\Delta\tilde{B}_i\tilde{F}_{jg}(x)C_j L & 0 & 0 & 0 & 0 & 0 \\ 0 & 0 & 0 & 0 & 0 & 0 & 0 \\ 0 & 0 & 0 & 0 & 0 & 0 & 0 \\ 0 & 0 & 0 & 0 & 0 & 0 & 0 \\ 0 & 0 & 0 & 0 & 0 & 0 & 0 \end{bmatrix}$$
$$+ \begin{bmatrix} -G_g(\tilde{x})\Delta\tilde{A}_i & -G_g(\tilde{x})\Delta\tilde{B}_i\tilde{F}_{jg}(x)C_j L & 0 & 0 & 0 & 0 & 0 \\ -G_g(\tilde{x})\Delta\tilde{A}_i & -G_g(\tilde{x})\Delta\tilde{B}_i\tilde{F}_{jg}(x)C_j L & 0 & 0 & 0 & 0 & 0 \\ -G_g(\tilde{x})\Delta\tilde{A}_i & -G_g(\tilde{x})\Delta\tilde{B}_i\tilde{F}_{jg}(x)C_j L & 0 & 0 & 0 & 0 & 0 \\ 0 & 0 & 0 & 0 & 0 & 0 & 0 \\ 0 & 0 & 0 & 0 & 0 & 0 & 0 \\ 0 & 0 & 0 & 0 & 0 & 0 & 0 \\ 0 & 0 & 0 & 0 & 0 & 0 & 0 \end{bmatrix}^T \quad (85)$$

Based on (85), the formula can as follows:

$$\Delta\tilde{\Phi}_{ijg}(x) = \begin{bmatrix} -G_g(\tilde{x}) \\ -G_g(\tilde{x}) \\ -G_g(\tilde{x}) \\ 0 \\ 0 \\ 0 \\ 0 \end{bmatrix} \begin{bmatrix} \Delta\tilde{A}_i & \Delta\tilde{B}_i\tilde{F}_{jg}(x)\tilde{C}_j L & 0 & 0 & 0 & 0 & 0 \end{bmatrix}$$
$$+ \begin{bmatrix} \Delta\tilde{A}_i & \Delta\tilde{B}_i\tilde{F}_{jg}(x)\tilde{C}_j L & 0 & 0 & 0 & 0 & 0 \end{bmatrix}^T \begin{bmatrix} -G_g(\tilde{x}) \\ -G_g(\tilde{x}) \\ -G_g(\tilde{x}) \\ 0 \\ 0 \\ 0 \\ 0 \end{bmatrix}^T \quad (86)$$

Form (7), we can rewrite (86) as (87)

$$\hat{\boldsymbol{\Phi}}_{ijg}(\boldsymbol{x})+\begin{bmatrix}-\boldsymbol{G}_g(\tilde{x})\\-\boldsymbol{G}_g(\tilde{x})\\-\boldsymbol{G}_g(\tilde{x})\\0\\0\\0\\0\end{bmatrix}\begin{bmatrix}\boldsymbol{JK}(t)\boldsymbol{R}_{ai} & \boldsymbol{JK}(t)\boldsymbol{R}_{bi}\tilde{\boldsymbol{F}}_{jg}(x)\tilde{\boldsymbol{C}}_j\boldsymbol{L} & 0 & 0 & 0 & 0 & 0\end{bmatrix}$$

$$+\begin{bmatrix}\boldsymbol{JK}(t)\boldsymbol{R}_{ai} & \boldsymbol{JK}(t)\boldsymbol{R}_{bi}\tilde{\boldsymbol{F}}_{jg}(x)\tilde{\boldsymbol{C}}_j\boldsymbol{L} & 0 & 0 & 0 & 0 & 0\end{bmatrix}^T\begin{bmatrix}-\boldsymbol{G}_g(\tilde{x})\\-\boldsymbol{G}_g(\tilde{x})\\-\boldsymbol{G}_g(\tilde{x})\\0\\0\\0\\0\end{bmatrix}^T<0 \tag{87}$$

Considering the model uncertainties are satisfied (7), there exists

$$\hat{\boldsymbol{\Phi}}_{ijg}(\boldsymbol{x})+\boldsymbol{PK}(t)\boldsymbol{Q}+\boldsymbol{Q}^T\boldsymbol{K}(t)\boldsymbol{P}^T<\boldsymbol{0} \tag{88}$$

where

$\boldsymbol{P}=\begin{bmatrix}-\boldsymbol{G}_g(\tilde{x})\tilde{\boldsymbol{J}} & -\boldsymbol{G}_g(\tilde{x})\tilde{\boldsymbol{J}} & -\boldsymbol{G}_g(\tilde{x})\tilde{\boldsymbol{J}} & 0 & 0 & 0 & 0\end{bmatrix}^T$,

$\boldsymbol{Q}=\begin{bmatrix}\tilde{\boldsymbol{R}}_{ai} & \tilde{\boldsymbol{R}}_{bi}\tilde{\boldsymbol{F}}_{jg}(\boldsymbol{x})\boldsymbol{C}_j\boldsymbol{L} & 0 & 0 & 0 & 0 & 0\end{bmatrix}$,

$\tilde{\boldsymbol{J}}=\boldsymbol{L}^{-1}\boldsymbol{J}$, $\tilde{\boldsymbol{R}}_{ai}=\boldsymbol{R}_{ai}\boldsymbol{L}$, $\tilde{\boldsymbol{R}}_{bi}=\boldsymbol{R}_{bi}$.

Utilizing Lemma 5, statement (88) implies the existence of positive scalars κ such that

$$\hat{\boldsymbol{\Phi}}_{ijg}(\boldsymbol{x})+\kappa^{-1}\boldsymbol{PP}^T+\kappa\boldsymbol{Q}^T\boldsymbol{Q}<\boldsymbol{0} \tag{89}$$

Applying the Schur complement again, it can be concluded that (89) is equivalent to

$$\boldsymbol{\Phi}_{ijg}(x)=\begin{bmatrix}\hat{\boldsymbol{\Phi}}_{ijg}(x) & \boldsymbol{P} & \kappa\boldsymbol{Q}^T\\ * & -\kappa\mathbf{I} & 0\\ * & * & -\kappa\mathbf{I}\end{bmatrix}<\boldsymbol{0} \tag{90}$$

Next, multiply (90) form left by $diag\left(\boldsymbol{G}_g^{-1}(\tilde{x}),\boldsymbol{G}_g^{-1}(\tilde{x}),\boldsymbol{G}_g^{-1}(\tilde{x}),\boldsymbol{G}_g^{-1}(\tilde{x}),\boldsymbol{I},\boldsymbol{G}_g^{-1}(\tilde{x}),\boldsymbol{I}\right)$ and right by its transpose, respectively, respectively.Setting $\boldsymbol{C}_j\boldsymbol{L}=\boldsymbol{I}$ $\boldsymbol{X}_g(\tilde{\boldsymbol{x}})=\boldsymbol{G}_g^{-T}(\tilde{\boldsymbol{x}})$, $\boldsymbol{F}_{jg}(\boldsymbol{x})=\boldsymbol{M}_{jg}(\boldsymbol{x})\boldsymbol{X}_g^{-1}(\tilde{\boldsymbol{x}})$, and replacing $\boldsymbol{G}_g^{-1}(\tilde{\boldsymbol{x}})\boldsymbol{P}_g(\tilde{\boldsymbol{x}})\boldsymbol{G}_g^{-1}(\tilde{\boldsymbol{x}})$, $\boldsymbol{G}_g^{-1}(\tilde{\boldsymbol{x}})\sum_{l\in\boldsymbol{L}}\frac{\partial\boldsymbol{P}_g}{\partial x_l}(\tilde{\boldsymbol{x}})\tilde{\boldsymbol{A}}_i^l(\boldsymbol{x})\hat{\boldsymbol{x}}\boldsymbol{G}_g^{-T}(\tilde{\boldsymbol{x}})$, $\boldsymbol{G}_g^{-1}(\tilde{\boldsymbol{x}})\boldsymbol{Q}_g(\boldsymbol{x})\boldsymbol{G}_g^{-1}(\tilde{\boldsymbol{x}})$, $\boldsymbol{G}_g^{-1}(\tilde{\boldsymbol{x}})\boldsymbol{R}_g(\boldsymbol{x})\boldsymbol{G}_g^{-1}(\tilde{\boldsymbol{x}})$ and $\boldsymbol{G}_g^{-1}(\tilde{\boldsymbol{x}})\boldsymbol{H}_{jg}(\boldsymbol{x})\boldsymbol{G}_g^{-1}(\tilde{\boldsymbol{x}})$ with $\boldsymbol{P}_g(\tilde{\boldsymbol{x}})$, $\sum_{l\in\boldsymbol{L}}\frac{\partial\boldsymbol{P}_g}{\partial x_l}(\tilde{\boldsymbol{x}})\tilde{\boldsymbol{A}}_i^l(\boldsymbol{x})\hat{\boldsymbol{x}}$, $\boldsymbol{Q}_g(\boldsymbol{x})$, $\boldsymbol{R}_g(\boldsymbol{x})$ and $\boldsymbol{H}_{jg}(\boldsymbol{x})(j=1,2,3)$, respectively. The stability conditions can be divided into $\boldsymbol{\Phi}_{ijg}(\boldsymbol{x})<0$ by using the replaced matrix. Therefore, if (26) are satisfied, it can guarantee that the novel piecewise polynomial fuzzy networked controller based on static output feedback can stabilize the closed-loop novel piecewise polynomial fuzzy networked control time-delay systems with both external disturbances and model uncertainties. Q.E.D.

(b) Proof2:

This is the derivation of the stability theorem of Theorem 2.

Take Lyapunov-Krasovskii piecewise polynomials functional as

$$\boldsymbol{V}_g(z_f)=z^{\mathrm{T}}\boldsymbol{P}_g(\tilde{x}_f)z_f+\int_{-\lambda}^{0}\int_{t+\omega}^{t}\dot{z}_f^{\mathrm{T}}(\sigma)\boldsymbol{Q}_g(\boldsymbol{x}_f)\dot{z}_f(\sigma)\mathrm{d}\sigma\mathrm{d}\omega \tag{91}$$

Using the Newton-Leibniz formula $\boldsymbol{z}_{fk}=\boldsymbol{z}_f-\int_{t_k}^{t}\dot{\boldsymbol{z}}_f(\boldsymbol{\sigma})d\sigma$, it is evident that, for any polynomial matrix $\boldsymbol{H}_{jg}(\boldsymbol{x}_f)(j=1,2,3)$ with the appropriate dimensions, we get

$$\left[z_f-z_{fk}-\int_{t_k}^{t}\dot{z}_f(\sigma)\mathrm{d}\sigma\right]^{\mathrm{T}}\times\left[\boldsymbol{H}_{1g}^{\mathrm{T}}(\boldsymbol{x}_f)z_f+\boldsymbol{H}_{2g}^{\mathrm{T}}(\boldsymbol{x}_f)z_{fk}+\boldsymbol{H}_{3g}^{\mathrm{T}}(\boldsymbol{x}_f)\dot{z}_f\right]=0 \tag{92}$$

$$\left[\boldsymbol{H}_{1g}^{\mathrm{T}}(\boldsymbol{x}_f)z_f+\boldsymbol{H}_{2g}^{\mathrm{T}}(\boldsymbol{x}_f)z_{fk}+\boldsymbol{H}_{3g}^{\mathrm{T}}(\boldsymbol{x}_f)\dot{z}_f\right]^{\mathrm{T}}\times\left[z_f-z_{fk}-\int_{t_k}^{t}\dot{z}_f(\sigma)\mathrm{d}\sigma\right]=0 \tag{93}$$

Furthermore, based on (16), we can derive nonsingular matrix $\boldsymbol{G}_g(\tilde{\boldsymbol{x}}_f)$ as follows:

$$\begin{aligned}&\left[\boldsymbol{G}_g^{\mathrm{T}}(\tilde{x}_f)z_f+\boldsymbol{G}_g^{\mathrm{T}}(\tilde{x}_f)z_{fk}+\boldsymbol{G}_g^{\mathrm{T}}(\tilde{x}_f)\dot{z}_f\right]^T\\&\times\left\{\dot{z}_f-\sum_{i=1}^{r}\sum_{j=1}^{r}s_is_j^k\left\{\begin{matrix}\left[\bar{\boldsymbol{A}}_i(\boldsymbol{x}_f)+\Delta\bar{\boldsymbol{A}}_i\right]z_f+\left[\bar{\boldsymbol{B}}_i(\boldsymbol{x}_f)+\Delta\bar{\boldsymbol{B}}_i\right]\boldsymbol{F}_{jg}(\boldsymbol{x}_f)\boldsymbol{C}_j\boldsymbol{L}z_{fk}\\+\bar{\boldsymbol{D}}_i(\boldsymbol{x}_f)\boldsymbol{v}\end{matrix}\right\}\right\}=0\end{aligned} \tag{94}$$

$$\begin{aligned}&\left\{\dot{z}_f-\sum_{i=1}^{r}\sum_{j=1}^{r}s_is_j^k\left\{\begin{matrix}\left[\bar{\boldsymbol{A}}_i(\boldsymbol{x}_f)+\Delta\bar{\boldsymbol{A}}_i\right]z_f+\left[\bar{\boldsymbol{B}}_i(\boldsymbol{x}_f)+\Delta\bar{\boldsymbol{B}}_i\right]\boldsymbol{F}_{jg}(\boldsymbol{x}_f)\boldsymbol{C}_j\boldsymbol{L}z_{fk}\\+\bar{\boldsymbol{D}}_i(\boldsymbol{x}_f)\boldsymbol{v}\end{matrix}\right\}\right\}^T\\&\times\left[\boldsymbol{G}_g^{\mathrm{T}}(\tilde{x}_f)z_f+\boldsymbol{G}_g^{\mathrm{T}}(\tilde{x}_f)z_{fk}+\boldsymbol{G}_g^{\mathrm{T}}(\tilde{x}_f)\dot{z}_f\right]=0\end{aligned} \tag{95}$$

The time derivative of $\boldsymbol{P}_g(\tilde{\boldsymbol{x}}_f)$ can be derived as follows:

$$\dot{\boldsymbol{P}}_g(\tilde{\boldsymbol{x}}_f)=\sum_{l\in L}\frac{\partial\boldsymbol{P}_g}{\partial x_l}(\tilde{\boldsymbol{x}}_f)\bar{\boldsymbol{A}}_i^l(\boldsymbol{x}_f)\bar{x}_f \tag{96}$$

Since $\tilde{\boldsymbol{B}}_i^l(\boldsymbol{x}_f)=0$ for $l\in\boldsymbol{L}$, the following equation can be obtained:

$$\dot{\boldsymbol{x}}_l=\sum_{i=1}^{r}s_i\bar{\boldsymbol{A}}_i^l(\boldsymbol{x}_f)\bar{\boldsymbol{x}}_f \tag{97}$$

On the other hand

$$\frac{\partial\boldsymbol{P}_g}{\partial x_l}(\tilde{\boldsymbol{x}}_f)=0 \tag{98}$$

Combining (91)–(96), the time derivative of $\boldsymbol{V}_g(z_f)$, for $t\in\left[t_k+\tau_k,t_{k+q}+\tau_{k+q}\right)$ is obtained as

$$\begin{aligned}\dot{V}_g(z_f)\le{}&\dot{z}_f^T\boldsymbol{P}_g(\tilde{x}_f)z_f+z_f^T\boldsymbol{P}_g(\tilde{x}_f)\dot{z}_f+z_f^T\dot{\boldsymbol{P}}_g(\tilde{x}_f)z_f+\lambda\dot{z}_f^T\boldsymbol{Q}_g(\boldsymbol{x}_f)\dot{z}_f\\&-\int_{t-\lambda}^{t}\dot{z}_f^T(\sigma)\boldsymbol{Q}_g(\boldsymbol{x}_f)\dot{z}_f(\sigma)d\sigma\\&+\left[z_f-z_{fk}-\int_{t_k}^{t}\dot{z}_f(\sigma)d\sigma\right]^T\times\left[\boldsymbol{H}_{1g}^T(\boldsymbol{x}_f)z_f+\boldsymbol{H}_{2g}^T(\boldsymbol{x}_f)z_{fk}+\boldsymbol{H}_{3g}^T(\boldsymbol{x}_f)\dot{z}_f\right]\\&+\left[\boldsymbol{H}_{1g}^T(\boldsymbol{x}_f)z_f+\boldsymbol{H}_{2g}^T(\boldsymbol{x}_f)z_{fk}+\boldsymbol{H}_{3g}^T(\boldsymbol{x}_f)\dot{z}_f\right]^T\times\left[z_f-z_{fk}-\int_{t_k}^{t}\dot{z}_f(\sigma)d\sigma\right]\\&+\left[\boldsymbol{G}_g^T(\tilde{x}_f)z_f+\boldsymbol{G}_g^T(\tilde{x}_f)z_{fk}+\boldsymbol{G}_g^T(\tilde{x}_f)\dot{z}_f\right]^T\\&\times\left\{\dot{z}_f-\sum_{i=1}^{r}\sum_{j=1}^{r}s_is_j^k\left\{\begin{matrix}\left[\bar{\boldsymbol{A}}_i(\boldsymbol{x}_f)+\Delta\bar{\boldsymbol{A}}_i\right]z_f+\left[\bar{\boldsymbol{B}}_i(\boldsymbol{x}_f)+\Delta\bar{\boldsymbol{B}}_i\right]\boldsymbol{F}_{jg}(\boldsymbol{x}_f)\boldsymbol{C}_j\boldsymbol{L}z_{fk}\\+\bar{\boldsymbol{D}}_i(\boldsymbol{x}_f)\boldsymbol{v}\end{matrix}\right\}\right\}\\&+\left\{\dot{z}_f-\sum_{i=1}^{r}\sum_{j=1}^{r}s_is_j^k\left\{\begin{matrix}\left[\bar{\boldsymbol{A}}_i(\boldsymbol{x}_f)+\Delta\bar{\boldsymbol{A}}_i\right]z_f+\left[\bar{\boldsymbol{B}}_i(\boldsymbol{x}_f)+\Delta\bar{\boldsymbol{B}}_i\right]\boldsymbol{F}_{jg}(\boldsymbol{x}_f)\boldsymbol{C}_j\boldsymbol{L}z_{fk}\\+\bar{\boldsymbol{D}}_i(\boldsymbol{x}_f)\boldsymbol{v}\end{matrix}\right\}\right\}^T\\&\times\left[\boldsymbol{G}_g^T(\tilde{x}_f)z_f+\boldsymbol{G}_g^T(\tilde{x}_f)z_{fk}+\boldsymbol{G}_g^T(\tilde{x}_f)\dot{z}_f\right]\\&+\sum_{g=1}^{N}\lambda_g\bar{x}_f^T\left(\boldsymbol{P}_q(\tilde{x}_f)-\boldsymbol{P}_g(\tilde{x}_f)\right)\bar{x}_f\end{aligned} \tag{99}$$

Utilizing *Lemma 1*, *Lemma 2* and *Lemma 3*, (92) and (93) can be derived as

$$
\begin{aligned}
&-\left[\boldsymbol{H}_{1g}^{T}\left(\boldsymbol{x}_f\right)z_f+\boldsymbol{H}_{2g}^{T}\left(\boldsymbol{x}_f\right)z_{fk}+\boldsymbol{H}_{3g}^{T}\left(\boldsymbol{x}_f\right)\dot{z}_f\right]^T\times\int_{t_k}^{t}\dot{z}_f\left(\sigma\right)d\sigma\\
&-\int_{t_k}^{t}\dot{z}_f^{\,T}\left(\sigma\right)d\sigma\times\left[\boldsymbol{H}_{1g}^{T}\left(\boldsymbol{x}_f\right)z_f+\boldsymbol{H}_{2g}^{T}\left(\boldsymbol{x}_f\right)z_{fk}+\boldsymbol{H}_{3g}^{T}\left(\boldsymbol{x}_f\right)\dot{z}_f\right]\\
&\le\lambda\eta^T\bar{\boldsymbol{H}}_g\left(\boldsymbol{x}_f\right)\boldsymbol{Q}_g^{-1}\left(\boldsymbol{x}_f\right)\bar{\boldsymbol{H}}_g^{T}\left(\boldsymbol{x}_f\right)\eta+\frac{1}{\lambda}\left(\int_{t_k}^{t}\dot{z}_f\left(\sigma\right)d\sigma\right)^T\boldsymbol{Q}_g\left(\boldsymbol{x}_f\right)\left(\int_{t_k}^{t}\dot{z}_f\left(\sigma\right)d\sigma\right)\\
&\le\lambda\eta^T\bar{\boldsymbol{H}}_g\left(\boldsymbol{x}_f\right)\boldsymbol{Q}_g^{-1}\left(\boldsymbol{x}_f\right)\bar{\boldsymbol{H}}_g^{T}\left(\boldsymbol{x}_f\right)\eta+\frac{t-t_k}{\lambda}\int_{t_k}^{t}\dot{z}_f^{\,T}\left(\sigma\right)\boldsymbol{Q}_g\left(\boldsymbol{x}_f\right)\dot{z}_f\left(\sigma\right)d\sigma\\
&\le\lambda\eta^T\bar{\boldsymbol{H}}_g\left(\boldsymbol{x}_f\right)\boldsymbol{Q}_g^{-1}\left(\boldsymbol{x}_f\right)\bar{\boldsymbol{H}}_g^{T}\left(\boldsymbol{x}_f\right)\eta+\int_{t-\lambda}^{t}\dot{z}_f^{\,T}\left(\sigma\right)\boldsymbol{Q}_g\left(\boldsymbol{x}_f\right)\dot{z}_f\left(\sigma\right)d\sigma
\end{aligned}
\tag{100}
$$

where

$\bar{\boldsymbol{H}}_g^{\mathrm{T}}\left(\boldsymbol{x}_f\right)=\left[\boldsymbol{H}_{1g}^{\mathrm{T}}\quad\boldsymbol{H}_{2g}^{\mathrm{T}}\quad\boldsymbol{H}_{3g}^{\mathrm{T}}\quad 0\right]$, $\boldsymbol{\eta}^{\mathrm{T}}=\left[z_f^{\mathrm{T}}\quad z_{fk}^{\mathrm{T}}\quad\dot{z}_f^{\mathrm{T}}\quad v^{\mathrm{T}}\right]$, $\exists\lambda>0,\ \exists\boldsymbol{Q}_g>0$.

Substituting the result of (100) into (99), the inequality can be rewritten as follows:

$$
\begin{aligned}
\dot{V}_g\left(z_f\right)<\;&\dot{z}_f^T\boldsymbol{P}_g\left(\tilde{x}_f\right)z_f+z_f^T\boldsymbol{P}_g\left(\tilde{x}_f\right)\dot{z}_f+z_f^T\dot{\boldsymbol{P}}_g\left(\tilde{x}_f\right)z_f\\
&+\lambda\dot{z}_f^T\boldsymbol{Q}_g\left(\boldsymbol{x}_f\right)\dot{z}_f+\lambda\boldsymbol{\eta}^T\bar{\boldsymbol{H}}_g\left(\boldsymbol{x}_f\right)\boldsymbol{Q}_g^{-1}\left(\boldsymbol{x}_f\right)\bar{\boldsymbol{H}}_g^T\left(\boldsymbol{x}_f\right)\boldsymbol{\eta}\\
&-\int_{t-\lambda}^{t}\dot{z}_f^T(\sigma)\boldsymbol{Q}_g\left(\boldsymbol{x}_f\right)\dot{z}_f(\sigma)d\sigma+\int_{t-\lambda}^{t}\dot{z}_f^T(\sigma)\boldsymbol{Q}_g\left(\boldsymbol{x}_f\right)\dot{z}_f(\sigma)d\sigma\\
&+\left[z_f-z_{fk}\right]^T\left[\boldsymbol{H}_{1g}^T\left(\boldsymbol{x}_f\right)z_f+\boldsymbol{H}_{2g}^T\left(\boldsymbol{x}_f\right)z_{fk}+\boldsymbol{H}_{3g}^T\left(\boldsymbol{x}_f\right)\dot{z}_f\right]\\
&+\left[\boldsymbol{H}_{1g}^T\left(\boldsymbol{x}_f\right)z_f+\boldsymbol{H}_{2g}^T\left(\boldsymbol{x}_f\right)z_{fk}+\boldsymbol{H}_{3g}^T\left(\boldsymbol{x}_f\right)\dot{z}_f\right]^T\left[z_f-z_{fk}\right]\\
&+\left[\boldsymbol{G}_g^T\left(\tilde{x}_f\right)z_f+\boldsymbol{G}_g^T\left(\tilde{x}_f\right)z_{fk}+\boldsymbol{G}_g^T\left(\tilde{x}_f\right)\dot{z}_f\right]^T\\
&\times\left\{\dot{z}_f-\sum_{i=1}^{r}\sum_{j=1}^{r}s_is_j^k\left\{\begin{matrix}\left[\bar{A}_i\left(\boldsymbol{x}_f\right)+\Delta\bar{A}_i\right]z_f+\left[\bar{\boldsymbol{B}}_i\left(\boldsymbol{x}_f\right)+\Delta\bar{\boldsymbol{B}}_i\right]\boldsymbol{F}_{jg}\left(\boldsymbol{x}_f\right)\boldsymbol{C}_j\boldsymbol{L}z_{fk}\\+\tilde{\boldsymbol{D}}_i(\boldsymbol{x}_f)\boldsymbol{v}\end{matrix}\right\}\right\}\\
&+\left\{\dot{z}_f-\sum_{i=1}^{r}\sum_{j=1}^{r}s_is_j^k\left\{\begin{matrix}\left[\bar{A}_i\left(\boldsymbol{x}_f\right)+\Delta\bar{A}_i\right]z_f+\left[\bar{\boldsymbol{B}}_i\left(\boldsymbol{x}_f\right)+\Delta\bar{\boldsymbol{B}}_i\right]\boldsymbol{F}_{jg}\left(\boldsymbol{x}_f\right)\boldsymbol{C}_j\boldsymbol{L}z_{fk}\\+\tilde{\boldsymbol{D}}_i(\boldsymbol{x}_f)\boldsymbol{v}\end{matrix}\right\}\right\}^T\\
&\times\left[\boldsymbol{G}_g^T\left(\tilde{x}_f\right)z_f+\boldsymbol{G}_g^T\left(\tilde{x}_f\right)z_{fk}+\boldsymbol{G}_g^T\left(\tilde{x}_f\right)\dot{z}_f\right]\\
&+\sum_{g=1}^{N}\lambda_g\bar{x}_f^T\left(\boldsymbol{P}_g\left(\tilde{x}_f\right)-\boldsymbol{P}_q\left(\tilde{x}_f\right)\right)\bar{x}_f
\end{aligned}
\tag{101}
$$

Moreover, the inequality can be reorganized by rewriting (101) with η as follows:

$$
\begin{aligned}
\dot{V}_g\left(z_f\right)<\sum_{i=1}^{r}\sum_{j=1}^{r}s_is_j^k\{&\\
&\eta^T\begin{bmatrix}\sum_{l\in\boldsymbol{L}}\frac{\partial\boldsymbol{P}_g}{\partial\boldsymbol{x}_l}\left(\tilde{x}_f\right)\tilde{A}_i^l(\boldsymbol{x}_f)\bar{x}_f+\sum_{g=1}^{N}\lambda_g\boldsymbol{L}^T\left[\boldsymbol{P}_q\left(\tilde{x}_f\right)-\boldsymbol{P}_g\left(\tilde{x}_f\right)\right]\boldsymbol{L} & 0 & \boldsymbol{P}_g\left(\tilde{x}_f\right)\\ 0 & 0 & \lambda\boldsymbol{Q}_g\left(\boldsymbol{x}_f\right)\\ \boldsymbol{P}_g\left(\tilde{x}_f\right) & 0 & 0\end{bmatrix}\eta\\
&+\eta^T\begin{bmatrix}\boldsymbol{H}_{1g}\left(\boldsymbol{x}_f\right) & -\boldsymbol{H}_{1g}\left(\boldsymbol{x}_f\right) & 0\\ \boldsymbol{H}_{2g}\left(\boldsymbol{x}_f\right) & -\boldsymbol{H}_{2g}\left(\boldsymbol{x}_f\right) & 0\\ \boldsymbol{H}_{3g}\left(\boldsymbol{x}_f\right) & -\boldsymbol{H}_{3g}\left(\boldsymbol{x}_f\right) & 0\end{bmatrix}\eta+\eta^T\begin{bmatrix}\boldsymbol{H}_{1g}\left(\boldsymbol{x}_f\right) & -\boldsymbol{H}_{1g}\left(\boldsymbol{x}_f\right) & 0\\ \boldsymbol{H}_{2g}\left(\boldsymbol{x}_f\right) & -\boldsymbol{H}_{2g}\left(\boldsymbol{x}_f\right) & 0\\ \boldsymbol{H}_{3g}\left(\boldsymbol{x}_f\right) & -\boldsymbol{H}_{3g}\left(\boldsymbol{x}_f\right) & 0\end{bmatrix}^T\eta\\
&+\boldsymbol{\eta}^T\begin{bmatrix}-\boldsymbol{G}_g\left(\tilde{x}_f\right)\left[\bar{A}_i\left(\boldsymbol{x}_f\right)+\Delta\bar{A}_i\right] & -\boldsymbol{G}_g\left(\tilde{x}_f\right)\left[\bar{\boldsymbol{B}}_i\left(\boldsymbol{x}_f\right)+\Delta\bar{\boldsymbol{B}}_i\right]\boldsymbol{F}_{jg}\left(\boldsymbol{x}_f\right)\boldsymbol{C}_j\boldsymbol{L} & \boldsymbol{G}_g\left(\tilde{x}_f\right) & 0\\ -\boldsymbol{G}_g\left(\tilde{x}_f\right)\left[\bar{A}_i\left(\boldsymbol{x}_f\right)+\Delta\bar{A}_i\right] & -\boldsymbol{G}_g\left(\tilde{x}_f\right)\left[\bar{\boldsymbol{B}}_i\left(\boldsymbol{x}_f\right)+\Delta\bar{\boldsymbol{B}}_i\right]\boldsymbol{F}_{jg}\left(\boldsymbol{x}_f\right)\boldsymbol{C}_j\boldsymbol{L} & \boldsymbol{G}_g\left(\tilde{x}_f\right) & 0\\ -\boldsymbol{G}_g\left(\tilde{x}_f\right)\left[\bar{A}_i\left(\boldsymbol{x}_f\right)+\Delta\bar{A}_i\right] & -\boldsymbol{G}_g\left(\tilde{x}_f\right)\left[\bar{\boldsymbol{B}}_i\left(\boldsymbol{x}_f\right)+\Delta\bar{\boldsymbol{B}}_i\right]\boldsymbol{F}_{jg}\left(\boldsymbol{x}_f\right)\boldsymbol{C}_j\boldsymbol{L} & \boldsymbol{G}_g\left(\tilde{x}_f\right) & 0\\ 0 & 0 & 0 & 0\end{bmatrix}\boldsymbol{\eta}\\
&+\boldsymbol{\eta}^T\begin{bmatrix}-\boldsymbol{G}_g\left(\tilde{x}_f\right)\left[\bar{A}_i\left(\boldsymbol{x}_f\right)+\Delta\bar{A}_i\right] & -\boldsymbol{G}_g\left(\tilde{x}_f\right)\left[\bar{\boldsymbol{B}}_i\left(\boldsymbol{x}_f\right)+\Delta\bar{\boldsymbol{B}}_i\right]\boldsymbol{F}_{jg}\left(\boldsymbol{x}_f\right)\boldsymbol{C}_j\boldsymbol{L} & \boldsymbol{G}_g\left(\tilde{x}_f\right) & 0\\ -\boldsymbol{G}_g\left(\tilde{x}_f\right)\left[\bar{A}_i\left(\boldsymbol{x}_f\right)+\Delta\bar{A}_i\right] & -\boldsymbol{G}_g\left(\tilde{x}_f\right)\left[\bar{\boldsymbol{B}}_i\left(\boldsymbol{x}_f\right)+\Delta\bar{\boldsymbol{B}}_i\right]\boldsymbol{F}_{jg}\left(\boldsymbol{x}_f\right)\boldsymbol{C}_j\boldsymbol{L} & \boldsymbol{G}_g\left(\tilde{x}_f\right) & 0\\ -\boldsymbol{G}_g\left(\tilde{x}_f\right)\left[\bar{A}_i\left(\boldsymbol{x}_f\right)+\Delta\bar{A}_i\right] & -\boldsymbol{G}_g\left(\tilde{x}_f\right)\left[\bar{\boldsymbol{B}}_i\left(\boldsymbol{x}_f\right)+\Delta\bar{\boldsymbol{B}}_i\right]\boldsymbol{F}_{jg}\left(\boldsymbol{x}_f\right)\boldsymbol{C}_j\boldsymbol{L} & \boldsymbol{G}_g\left(\tilde{x}_f\right) & 0\\ 0 & 0 & 0 & 0\end{bmatrix}^T\boldsymbol{\eta}\\
&+\lambda\eta^T\bar{\boldsymbol{H}}_g\left(\boldsymbol{x}_f\right)\boldsymbol{Q}_g^{-1}\left(\boldsymbol{x}_f\right)\bar{\boldsymbol{H}}_g^T\left(\boldsymbol{x}_f\right)\eta\}
\end{aligned}
\tag{102}
$$

Rewrite (102) into the form as follows:

$$
\dot{V}_g\left(z_f\right)<\sum_{i=1}^{r}\sum_{j=1}^{r}s_is_j^k\eta^T\left[\boldsymbol{\Xi}_{ijg}+\lambda\bar{\boldsymbol{H}}_g\left(\boldsymbol{x}_f\right)\boldsymbol{Q}_g^{-1}\left(\boldsymbol{x}_f\right)\bar{\boldsymbol{H}}_g^T\left(\boldsymbol{x}_f\right)\right]\eta
\tag{103}
$$

where

$$
\boldsymbol{\Xi}_{ijg}=\begin{bmatrix}\bar{\boldsymbol{\Xi}}_{11g}+\boldsymbol{L}^{\mathrm{T}}\boldsymbol{C}_{\mathrm{i}}^{\mathrm{T}}\boldsymbol{C}_{\mathrm{i}}\boldsymbol{L} & \bar{\boldsymbol{\Xi}}_{12g} & \bar{\boldsymbol{\Xi}}_{13g} & -\boldsymbol{G}_{\mathrm{g}}\left(\tilde{\boldsymbol{x}}_f\right)\tilde{\boldsymbol{D}}_{\mathrm{i}}(\boldsymbol{x}_f(\mathrm{t}))\\ * & \bar{\boldsymbol{\Xi}}_{22g} & \bar{\boldsymbol{\Xi}}_{23g} & -\boldsymbol{G}_{\mathrm{g}}\left(\tilde{\boldsymbol{x}}_f\right)\tilde{\boldsymbol{D}}_{\mathrm{i}}(\boldsymbol{x}_f(\mathrm{t}))\\ * & * & \bar{\boldsymbol{\Xi}}_{33g} & -\boldsymbol{G}_{\mathrm{g}}\left(\tilde{\boldsymbol{x}}_f\right)\tilde{\boldsymbol{D}}_{\mathrm{i}}(\boldsymbol{x}_f(\mathrm{t}))\\ * & * & * & -\gamma^2\boldsymbol{I}\end{bmatrix}
$$

$$
\begin{aligned}
\bar{\boldsymbol{\Xi}}_{11g}=&\sum_{l\in\boldsymbol{L}}\frac{\partial\boldsymbol{P}_g}{\partial x_l}\left(\tilde{\boldsymbol{x}}_f\right)\bar{A}_i^l\left(\boldsymbol{x}_f\right)\bar{\boldsymbol{x}}_f+\boldsymbol{H}_{1g}\left(\boldsymbol{x}_f\right)+\boldsymbol{H}_{1g}^T\left(\boldsymbol{x}_f\right)-\boldsymbol{G}_g\left(\tilde{\boldsymbol{x}}_f\right)\left[\bar{A}_i\left(\boldsymbol{x}_f\right)+\Delta\bar{A}_i\right]\\
&-\left[\bar{A}_i\left(\boldsymbol{x}_f\right)+\Delta\bar{A}_i\right]^T\boldsymbol{G}_g^T\left(\tilde{\boldsymbol{x}}_f\right)+\sum_{g=1}^{N}\lambda_g\boldsymbol{L}^T\left[\boldsymbol{P}_q\left(\tilde{\boldsymbol{x}}_f\right)-\boldsymbol{P}_g\left(\tilde{\boldsymbol{x}}_f\right)\right]\boldsymbol{L}\\
\bar{\boldsymbol{\Xi}}_{12g}=&\boldsymbol{H}_{2g}^T\left(\boldsymbol{x}_f\right)-\boldsymbol{H}_{1g}\left(\boldsymbol{x}_f\right)-\boldsymbol{G}_g\left(\tilde{\boldsymbol{x}}_f\right)\left[\bar{\boldsymbol{B}}_i\left(\boldsymbol{x}_f\right)+\Delta\bar{\boldsymbol{B}}_i\right]\boldsymbol{F}_{jg}\left(\boldsymbol{x}_f\right)\boldsymbol{C}_j\boldsymbol{L}-\left[\bar{A}_i\left(\boldsymbol{x}_f\right)+\Delta\bar{A}_i\right]^T\boldsymbol{G}_g^T\left(\tilde{\boldsymbol{x}}_f\right)\\
\bar{\boldsymbol{\Xi}}_{13g}=&\boldsymbol{P}_g\left(\tilde{\boldsymbol{x}}_f\right)+\boldsymbol{H}_{3g}^T\left(\boldsymbol{x}_f\right)+\boldsymbol{G}_g\left(\tilde{\boldsymbol{x}}_f\right)-\left[\bar{A}_i\left(\boldsymbol{x}_f\right)+\Delta\bar{A}_i\right]^T\boldsymbol{G}_g^T\left(\tilde{\boldsymbol{x}}_f\right)\\
\bar{\boldsymbol{\Xi}}_{22g}=&-\boldsymbol{H}_{2g}\left(\boldsymbol{x}_f\right)-\boldsymbol{H}_{2g}^T\left(\boldsymbol{x}_f\right)-\boldsymbol{G}_g\left(\tilde{\boldsymbol{x}}_f\right)\left[\bar{\boldsymbol{B}}_i\left(\boldsymbol{x}_f\right)+\Delta\bar{\boldsymbol{B}}_i\right]^T\left(\boldsymbol{x}_f\right)\boldsymbol{F}_{jg}\left(\boldsymbol{x}_f\right)\boldsymbol{C}_j\boldsymbol{L}\\
&-\boldsymbol{L}^T\boldsymbol{C}_j^T\boldsymbol{F}_{jg}^T\left(\boldsymbol{x}_f\right)\left[\bar{\boldsymbol{B}}_i\left(\boldsymbol{x}_f\right)+\Delta\bar{\boldsymbol{B}}_i\right]^T\left(\boldsymbol{x}_f\right)\boldsymbol{G}_g^T\left(\tilde{\boldsymbol{x}}_f\right)\\
\bar{\boldsymbol{\Xi}}_{23g}=&\boldsymbol{G}_g\left(\tilde{\boldsymbol{x}}_f\right)-\boldsymbol{H}_{3g}^T\left(\boldsymbol{x}_f\right)-\boldsymbol{L}^T\boldsymbol{C}_j^T\boldsymbol{F}_{jg}^T\left(\boldsymbol{x}_f\right)\left[\bar{\boldsymbol{B}}_i\left(\boldsymbol{x}_f\right)+\Delta\bar{\boldsymbol{B}}_i\right]^T\left(\boldsymbol{x}_f\right)\boldsymbol{G}_g^T\left(\tilde{\boldsymbol{x}}_f\right)\\
\bar{\boldsymbol{\Xi}}_{33g}=&\lambda\boldsymbol{Q}_g\left(\boldsymbol{x}_f\right)+\boldsymbol{G}_g\left(\tilde{\boldsymbol{x}}_f\right)+\boldsymbol{G}_g^T\left(\tilde{\boldsymbol{x}}_f\right)
\end{aligned}
$$

Consider H_∞ performance index such as (15). The following inequality can be expressed as

$$
\dot{\boldsymbol{V}}_g(\boldsymbol{x}_f)+\boldsymbol{y}^T\boldsymbol{y}-\gamma^2\boldsymbol{v}^T\boldsymbol{v}<0
\tag{104}
$$

Based on (102) and (104), the inequality is obtained as follows

$$
\sum_{i=1}^{r}\sum_{j=1}^{r}\mathrm{s_i s_j^k}\eta^{\mathrm{T}}\left[\boldsymbol{\Xi}_{ijg}+\lambda\bar{\boldsymbol{H}}_{\mathrm{g}}\left(\boldsymbol{x}_f\right)\boldsymbol{Q}_{\mathrm{g}}^{-1}\left(\boldsymbol{x}_f\right)\bar{\boldsymbol{H}}_{\mathrm{g}}^{\mathrm{T}}\left(\boldsymbol{x}_f\right)\right]\eta<0
\tag{105}
$$

If $\boldsymbol{\Xi}_{ijg}+\lambda\bar{\boldsymbol{H}}_{\mathrm{g}}\left(\boldsymbol{x}_f\right)\boldsymbol{Q}_{\mathrm{g}}^{-1}\left(\boldsymbol{x}_f\right)\bar{\boldsymbol{H}}_{\mathrm{g}}^{\mathrm{T}}\left(\boldsymbol{x}_f\right)<0$ is satisfied for $i\le j$, it means $\dot{\boldsymbol{V}}_g\left(z_f\right)<0$.

The inequality can be obtained as (106) by using the Schur complement.

$$
\dot{V}_g\left(z_f\right)<\sum_{i=1}^{r}\sum_{j=1}^{r}s_is_j^k\boldsymbol{\eta}^T\bar{\boldsymbol{\Phi}}_{ijg}(\boldsymbol{x}_f)\boldsymbol{\eta}
\tag{106}
$$

where

$$
\bar{\boldsymbol{\Phi}}_{ijg}(\boldsymbol{x}_f)=\begin{bmatrix}\bar{\boldsymbol{\Xi}}_{11g} & \bar{\boldsymbol{\Xi}}_{12g} & \bar{\boldsymbol{\Xi}}_{13g} & -\boldsymbol{G}_g\left(\tilde{x}_f\right)\tilde{\boldsymbol{D}}_i(\boldsymbol{x}_f(t)) & \lambda\boldsymbol{H}_{1g}(\boldsymbol{x}_f) & \boldsymbol{L}^T\boldsymbol{C}_i^T(\boldsymbol{x}_f)\\ * & \bar{\boldsymbol{\Xi}}_{22g} & \bar{\boldsymbol{\Xi}}_{23g} & -\boldsymbol{G}_g\left(\tilde{x}_f\right)\tilde{\boldsymbol{D}}_i(\boldsymbol{x}_f(t)) & \lambda\boldsymbol{H}_{2g}(\boldsymbol{x}_f) & 0\\ * & * & \bar{\boldsymbol{\Xi}}_{33g} & -\boldsymbol{G}_g\left(\tilde{x}_f\right)\tilde{\boldsymbol{D}}_i(\boldsymbol{x}_f(t)) & \lambda\boldsymbol{H}_{3g}(\boldsymbol{x}_f) & 0\\ * & * & * & -\gamma^2\boldsymbol{I} & 0 & 0\\ * & * & * & * & -\lambda\boldsymbol{Q}_g(\boldsymbol{x}_f) & 0\\ * & * & * & * & * & -\boldsymbol{I}\end{bmatrix}
\tag{107}
$$

The transposed matrix at the symmetrical position is denoted as *.

For brevity, $\tilde{\boldsymbol{\Phi}}_{ijg}(\boldsymbol{x}_f)$ will be separated into two parts. $\bar{\boldsymbol{\Phi}}_{ijg}(\boldsymbol{x}_f)$ is the term without model uncertainties. $\Delta\tilde{\boldsymbol{\Phi}}_{ijg}(\boldsymbol{x}_f)$ is the model uncertainties term. Thus

$$
\tilde{\boldsymbol{\Phi}}_{\mathrm{ijg}}(x_f)=\bar{\boldsymbol{\Phi}}_{\mathrm{ijg}}(x_f)+\Delta\tilde{\boldsymbol{\Phi}}_{\mathrm{ijg}}(x_f)
\tag{108}
$$

among them

$$
\bar{\boldsymbol{\Phi}}_{ijg}(\boldsymbol{x}_f)=\begin{bmatrix}\hat{\boldsymbol{\Xi}}_{11g} & \hat{\boldsymbol{\Xi}}_{12g} & \hat{\boldsymbol{\Xi}}_{13g} & -\boldsymbol{G}_g\left(\tilde{x}_f\right)\tilde{\boldsymbol{D}}_i(\boldsymbol{x}_f(t)) & \lambda\boldsymbol{H}_{1g}(\boldsymbol{x}_f) & \boldsymbol{L}^T\boldsymbol{C}_i^T(\boldsymbol{x}_f)\\ * & \hat{\boldsymbol{\Xi}}_{22g} & \hat{\boldsymbol{\Xi}}_{23g} & -\boldsymbol{G}_g\left(\tilde{x}_f\right)\tilde{\boldsymbol{D}}_i(\boldsymbol{x}_f(t)) & \lambda\boldsymbol{H}_{2g}(\boldsymbol{x}_f) & 0\\ * & * & \hat{\boldsymbol{\Xi}}_{33g} & -\boldsymbol{G}_g\left(\tilde{x}_f\right)\tilde{\boldsymbol{D}}_i(\boldsymbol{x}_f(t)) & \lambda\boldsymbol{H}_{3g}(\boldsymbol{x}_f) & 0\\ * & * & * & -\gamma^2\boldsymbol{I} & 0 & 0\\ * & * & * & * & -\lambda\boldsymbol{Q}_g(\boldsymbol{x}_f) & 0\\ * & * & * & * & * & -\boldsymbol{I}\end{bmatrix}
\tag{109}
$$

The transposed matrix at the symmetrical position is denoted as *.

$$\hat{\Xi}_{11g}=\sum_{l\in L}\frac{\partial P_g}{\partial x_l}\left(\tilde{x}_f\right)\bar{A}_i^l\left(x_f\right)\bar{x}+H_{1g}\left(x_f\right)+H_{1g}^T\left(x_f\right)-G_g\left(\tilde{x}_f\right)\bar{A}_i\left(x_f\right)$$
$$-\bar{A}_i\left(x_f\right)G_g^T\left(\tilde{x}_f\right)+\sum_{g=1}^{N}\lambda_g L^T\left[P_q\left(\tilde{x}_f\right)-P_g\left(\tilde{x}_f\right)\right]L$$
$$\hat{\Xi}_{12g}=H_{2g}^T\left(x_f\right)-H_{1g}\left(x_f\right)-G_g\left(\tilde{x}_f\right)\bar{B}_i^T\left(x_f\right)F_{jg}\left(x_f\right)C_jL-\bar{A}_i\left(x_f\right)G_g^T\left(\tilde{x}_f\right)$$
$$\hat{\Xi}_{13g}=P_g\left(\tilde{x}_f\right)+H_{3g}^T\left(x_f\right)+G_g\left(\tilde{x}_f\right)-\bar{A}_i\left(x_f\right)G_g^T\left(\tilde{x}_f\right)$$
$$\hat{\Xi}_{22g}=-H_{2g}\left(x_f\right)-H_{2g}^T\left(x_f\right)-G_g\left(\tilde{x}_f\right)\bar{B}_i^T\left(x_f\right)F_{jg}\left(x_f\right)C_jL$$
$$-L^TC_j^TF_{jg}^T\left(x_f\right)\bar{B}_i^T\left(x_f\right)G_g^T\left(\tilde{x}_f\right)$$
$$\hat{\Xi}_{23g}=G_g\left(\tilde{x}_f\right)-H_{3g}^T\left(x_f\right)-L^TC_j^TF_{jg}^T\left(x_f\right)\bar{B}_i^T\left(x_f\right)G_g^T\left(\tilde{x}_f\right)$$
$$\hat{\Xi}_{33g}=\lambda Q_g\left(x_f\right)+G_g\left(\tilde{x}_f\right)+G_g^T\left(\tilde{x}_f\right)$$

$$\Delta\tilde{\Phi}_{ijg}(x_f)=\begin{bmatrix}-G_g\left(\tilde{x}_f\right)\Delta\bar{A}_i & -G_g\left(\tilde{x}_f\right)\Delta\bar{B}_i\tilde{F}_{jg}\left(x_f\right)C_jL & 0 & 0 & 0 & 0\\ -G_g\left(\tilde{x}_f\right)\Delta\bar{A}_i & -G_g\left(\tilde{x}_f\right)\Delta\bar{B}_i\tilde{F}_{jg}\left(x_f\right)C_jL & 0 & 0 & 0 & 0\\ -G_g\left(\tilde{x}_f\right)\Delta\bar{A}_i & -G_g\left(\tilde{x}_f\right)\Delta\bar{B}_i\tilde{F}_{jg}\left(x_f\right)C_jL & 0 & 0 & 0 & 0\\ 0 & 0 & 0 & 0 & 0 & 0\\ 0 & 0 & 0 & 0 & 0 & 0\\ 0 & 0 & 0 & 0 & 0 & 0\end{bmatrix}\tag{110}$$
$$+\begin{bmatrix}-G_g\left(\tilde{x}_f\right)\Delta\bar{A}_i & -G_g\left(\tilde{x}_f\right)\Delta\bar{B}_i\tilde{F}_{jg}\left(x_f\right)C_jL & 0 & 0 & 0 & 0\\ -G_g\left(\tilde{x}_f\right)\Delta\bar{A}_i & -G_g\left(\tilde{x}_f\right)\Delta\bar{B}_i\tilde{F}_{jg}\left(x_f\right)C_jL & 0 & 0 & 0 & 0\\ -G_g\left(\tilde{x}_f\right)\Delta\bar{A}_i & -G_g\left(\tilde{x}_f\right)\Delta\bar{B}_i\tilde{F}_{jg}\left(x_f\right)C_jL & 0 & 0 & 0 & 0\\ 0 & 0 & 0 & 0 & 0 & 0\\ 0 & 0 & 0 & 0 & 0 & 0\\ 0 & 0 & 0 & 0 & 0 & 0\end{bmatrix}^T$$

Based on (110), the formula can as follows:

$$\Delta\tilde{\Phi}_{ijg}(x_f)=\begin{bmatrix}-G_g\left(\tilde{x}_f\right)\\-G_g\left(\tilde{x}_f\right)\\-G_g\left(\tilde{x}_f\right)\\0\\0\\0\end{bmatrix}\begin{bmatrix}\Delta\bar{A}_i & \Delta\bar{B}_i\tilde{F}_{jg}\left(x_f\right)\tilde{C}_jL & 0 & 0 & 0 & 0\end{bmatrix}\tag{111}$$
$$+\begin{bmatrix}\Delta\bar{A}_i & \Delta\bar{B}_i\tilde{F}_{jg}\left(x_f\right)\tilde{C}_jL & 0 & 0 & 0 & 0\end{bmatrix}^T\begin{bmatrix}-G_g\left(\tilde{x}_f\right)\\-G_g\left(\tilde{x}_f\right)\\-G_g\left(\tilde{x}_f\right)\\0\\0\\0\end{bmatrix}^T$$

Form (7), we can rewrite (111) as (112)

$$\bar{\Phi}_{ijg}(x_f)+\begin{bmatrix}-G_g\left(\tilde{x}_f\right)\\-G_g\left(\tilde{x}_f\right)\\-G_g\left(\tilde{x}_f\right)\\0\\0\\0\end{bmatrix}\begin{bmatrix}JK(t)R_{ai} & JK(t)R_{bi}\tilde{F}_{jg}\left(x_f\right)\tilde{C}_jL & 0 & 0 & 0 & 0\end{bmatrix}\tag{112}$$
$$+\begin{bmatrix}JK(t)R_{ai} & JK(t)R_{bi}\tilde{F}_{jg}\left(x_f\right)\tilde{C}_jL & 0 & 0 & 0 & 0\end{bmatrix}^T\begin{bmatrix}-G_g\left(\tilde{x}_f\right)\\-G_g\left(\tilde{x}_f\right)\\-G_g\left(\tilde{x}_f\right)\\0\\0\\0\end{bmatrix}^T<0$$

Considering the model uncertainties are satisfied (7), there exists

$$\bar{\Phi}_{ijg}(x_f)+PK(t)Q+Q^TK(t)P^T<\mathbf{0}\tag{113}$$

where

$P=\begin{bmatrix}-G_g\left(\tilde{x}_f\right)\tilde{J} & -G_g\left(\tilde{x}_f\right)\tilde{J} & -G_g\left(\tilde{x}_f\right)\tilde{J} & 0 & 0 & 0\end{bmatrix}^T$,

$Q=\begin{bmatrix}\tilde{R}_{ai} & \tilde{R}_{bi}\tilde{F}_{jg}\left(x_f\right)C_jL & 0 & 0 & 0 & 0\end{bmatrix}$,

$\tilde{J}=L^{-1}J$, $\tilde{R}_{ai}=R_{ai}L$, $\tilde{R}_{bi}=R_{bi}$.

Utilizing Lemma 5, statement (113) implies the existence of positive scalars κ such that

$$\bar{\Phi}_{ijg}(x_f)+\kappa^{-1}PP^T+\kappa Q^TQ<\mathbf{0}\tag{114}$$

Applying the Schur complement again, it can be concluded that (114) is equivalent to

$$\Phi_{ijg}(x_f)=\begin{bmatrix}\bar{\Phi}_{ijg}(x_f) & P & \kappa Q^T\\ * & -\kappa\mathbf{I} & 0\\ * & * & -\kappa\mathbf{I}\end{bmatrix}<\mathbf{0}\tag{115}$$

Next, multiply (115) form left by $diag\left(G_g^{-1}(\tilde{x}_f),G_g^{-1}(\tilde{x}_f),G_g^{-1}(\tilde{x}_f),G_g^{-1}(\tilde{x}_f),G_g^{-1}(\tilde{x}_f)\right)$ and right by its transpose, respectively, respectively.Setting $C_jL=I$ $X_g(\tilde{x}_f)=G_g^{-T}(\tilde{x}_f)$, $F_{jg}(x_f)=M_{jg}(x_f)X_g^{-1}(\tilde{x}_f)$, and replacing $G_g^{-1}\left(\tilde{x}_f\right)P_g\left(\tilde{x}_f\right)G_g^{-1}\left(\tilde{x}_f\right)$, $G_g^{-1}\left(\tilde{x}_f\right)\sum_{l\in L}\frac{\partial P_g}{\partial x_l}\left(\tilde{x}_f\right)\tilde{A}_i^l\left(x_f\right)\bar{x}_fG_g^{-T}\left(\tilde{x}_f\right)$, $G_g^{-1}\left(\tilde{x}_f\right)Q_g\left(x_f\right)G_g^{-1}\left(\tilde{x}_f\right)$ and $G_g^{-1}\left(\tilde{x}_f\right)H_{jg}\left(x_f\right)G_g^{-1}\left(\tilde{x}_f\right)$ with $P_g\left(\tilde{x}_f\right)$, $\sum_{l\in L}\frac{\partial P_g}{\partial x_l}\left(\tilde{x}_f\right)\tilde{A}_i^l\left(x_f\right)\bar{x}_f$, $Q_g\left(x_f\right)$ and $H_{jg}\left(x_f\right)\left(j=1,2,3\right)$, respectively. The stability conditions can be divided into $\Phi_{ijg}(x_f)<0$ by using the replaced matrix. Therefore, if (30) are satisfied, it can guarantee that the novel piecewise polynomial fuzzy networked controller based on static output feedback can stabilize the closed-loop novel piecewise polynomial fuzzy networked control time-delay systems with both external disturbances and model uncertainties.

Q.E.D.